

## FINAL REPORT

DURABILITY OF CERTAIN CONFIGURATIONS FOR  
PROVIDING SKID RESISTANCE ON CONCRETE PAVEMENTS

by

Celik Ozyildirim  
Graduate Assistant

(The opinions, findings, and conclusions expressed in this report are those of the author and not necessarily those of the sponsoring agency.)

Virginia Highway Research Council  
(A Cooperative Organization Sponsored Jointly by the Virginia  
Department of Highways and the University of Virginia)

In Cooperation with the U.S. Department of Transportation  
Federal Highway Administration

Charlottesville, Virginia

June 1974

VHRC 73-R57



## ABSTRACT

The main objective of this study was to establish the factors that influence the durability of the surface configurations that are used or can be used to provide high and long lasting skid resistance for portland cement concrete pavements. In the development of such durable surface texture an insight into the pavement wear mechanism in the presence of grooves is necessary. The wear of pavements may involve polishing and small-scale degradation at the top surface as well as a possible large-scale material loss.

The study of wear phenomena for rough textured concrete pavements involved the investigation of:

- (1) The surface behavior of the pavement, and
- (2) the structural behavior of the area below the top surface and around the grooves.

The wear phenomena occurring at the top surface was investigated experimentally by petrographic examination of thin sections prepared from the cores taken from actual highways that had experienced various degrees of wear. The samples included saw cut grooves imparted to the worn concrete surface, and also textures imparted to the fresh concrete pavements by burlap drag and metal tines.

The microscopic study of the thin sections showed that most of the cracks were found at the top surface and virtually no cracks were seen at the bottom of the grooves. Variation in the strength of the pastes affected the wear. The loss of material at the surface in strong pastes resulted from flaking, and in weaker pastes it was because of crushing. Both pastes yielded good microtexture, but the weaker mixtures wore faster. The chipping of aggregates at planes and zones of weakness also provided good microtexture.

Concrete slabs having different surface textures were prefabricated and tested on a circular test track. After 1,670,000 wheel passes, no appreciable wear was observed. This indicated that the surface pressures exerted by the tires used in the test track are low, and it takes a large number of wheel passes to wear the pavement surface.

The samples studied microscopically had a maximum groove depth of 1/8" (3.2mm), and it was noted that a large-scale material failure did not occur in the concrete and wear was mainly a surface phenomenon. However, deeper grooves might cause a structural failure as well as the ordinary surface wear.

The structural behavior of the area below the top surface and around the grooves was investigated theoretically. Involved was the determination of internal stresses within the concrete under an assumed surface loading. If the internal stresses were higher than the ultimate capacity of the material, cracks and eventual loss of material would occur at critical regions. This would indicate a large-scale failure. Initially three types of grooves, (square, triangular and round),

having a 1/8" (3.2mm) texture depth and 3/4" (19.0mm) spacing were considered. It was found that the critical locations where stresses could develop to cause failure were at the bottom or at the corner of the grooves. Later the effect of groove geometry on the internal stresses was investigated theoretically by considering the effect of increasing the depth of square grooves from 1/8" (3.2mm) to 1" (25.4mm) in 1/8" (3.2mm) increments while keeping the groove width and spacing constant. In this way deeper rectangular grooves were formed that provided better drainage. It is concluded that the deeper grooves are more prone to structural failure since increasing the depth of the groove yields higher principal tensile stresses.

The freezing and thawing durability of the square, triangular, and round groove configuration was satisfactory, and after 50 cycles no differences could be distinguished in the durability of the tested groove configurations.

## DURABILITY OF CERTAIN CONFIGURATIONS FOR PROVIDING SKID RESISTANCE ON CONCRETE PAVEMENTS

by  
Celik Ozyildirim  
Graduate Assistant

### THE PROBLEM

Skidding has been a serious problem in highway safety, and with the increase in traffic density, vehicle speed, and engine horsepower, the number of skid related accidents and their severity have risen. (1, 2, 3)\* A certain level of frictional resistance between the pavement surface and the vehicle tires is required for driving, steering, and braking vehicles. When a tire, prevented from rotating, slides along the pavement, the forces generated are called skid resistance. (4, 5) The provision and maintenance of satisfactory skid resistance are major concerns in highway engineering and safety.

### FACTORS THAT INFLUENCE SKID RESISTANCE

Tire-pavement friction, which is essential for the proper and safe performance of any highway, is a complex phenomenon. It is significantly affected by factors such as characteristics of the tire and the pavement surface, and operating conditions such as temperature, tire pressure, amount of water on the surface, and vehicle speed. The amounts of accumulated oil, worn rubber, loose dust, and grit on the surface also affect the friction. (5, 6) The two most important of these, the tire and the pavement surface factors are discussed below.

#### Tire Factors

The two principal components of rubber friction are adhesion and hysteresis. (4, 7, 8) Adhesion is caused by the energy dissipation resulting from the making and breaking of atomic bonds at the contact area. Hysteresis results from the damping losses in rubber compressed or expanded by the surface roughness.

The skid resistance of dry portland cement concrete pavements is satisfactory. However, when there is water or any other lubricant on the surface, the tire-pavement friction decreases considerably. On wet surfaces the adhesion component is reduced to a small value, whereas the hysteresis component shows little change. Therefore, many researchers state that the hysteresis component is the primary source of wet rubber friction. (9)

---

\*The numbers in parentheses denote items in the list of references

The hysteresis component of friction increases noticeably as the sliding speeds become high (say 50mph (80 km per hr) or above). (6) However, the adhesion component, which is important at low speeds, decreases as the speed increases. On wet pavements, increased vehicle speeds may result in a condition known as hydroplaning in which the tire rides up on the water that covers the surface and causes a loss of braking and steering capability. Hydroplaning is affected by the depth of fluid on the pavement, the surface texture, and the tire tread design. (10, 11, 12)

### Pavement Surface Factors

Surface texture—the macroscopic and microscopic roughnesses of the pavement surface—is the primary parameter of surface characteristics. The coarse macrotexture is formed by the finishing methods. A coarse texture provides drainage channels for water and imparts the hysteresis component of friction. The fine microtexture governs the adhesion component and provides the contact between the tire rubber and the pavement surface. A good skid resistant surface should include both fine and coarse textures.

A surface which originally yields satisfactory friction values may polish or disintegrate under the wear of traffic or the influence of the environment particularly freezing and thawing in the presence of deicing chemicals. It is desired that the surface retain its texture over the service life of the pavement.

In the past, concrete pavements as designed have served adequately as long as nonpolishing aggregates have been used and a moderate texture obtained. (13) The present traffic volumes and the increases in speeds have caused an accelerated rate of wear.

Under the present traffic conditions, a durable texture with comparatively large ridges of mortar has become a necessity. The rough texture can be imparted to the pavement surface either at the time of construction by the finishing methods or at a later date by sawing grooves into the worn surface. (14, 15, 16, 17) The grooves cut into the pavement usually have a uniform surface configuration. Those imparted to the highway at the time of construction may have randomly or uniformly rough surface textures, depending upon the finishing method. For example, textures established using a burlap drag or broom are of a random nature, whereas fairly uniform textures can be achieved using a magnesium fluted float or rotating drum.

A study by the New York State Department of Transportation revealed that uniformly rough textures applied during construction wear at a slower rate than irregular ones. The uniform textures were formed by the fluted float and had a texture depth equivalent to that of a wire broom. They were deeper than those produced by the burlap drag or the natural-bristle broom. This study found that the better performance of uniformly rough textures is probably due to reduced peak stresses and uniform curing. (18) The rough textures improve traction under wet conditions at high speeds. (4, 19) Deep textures can be longitudinal, transverse, or skewed. Longitudinal grooving is considered to increase the directional control of

the vehicle and causes the lowest noise level of the various orientations and is therefore used extensively. (20)

Although a considerable local and national research effort has been directed toward the problem of providing high skid resistance, definitive work on the mechanical response for portland cement concrete surfaces, particularly those incorporating very severe relief, has been lacking. A recent series of reports by the British Road Research Laboratory (17, 21, 22) constitutes the primary published effort in this field.

In Virginia, studies directed toward establishing optimum configurations are being conducted through field trials under the guidance of a committee including representatives of the Research Council and the Virginia Department of Highways' operating divisions. These studies are beyond the scope although related to this project, which is concerned with the wearability of various textures that might offer a high degree of skid resistance. On the basis of available published information and field experience, it is apparent that severe textures will be necessary to provide the needed frictional levels. The use of such textures naturally raises questions as to their durability.

#### PAVEMENT WEAR MECHANISM

The critical need is for a surface configuration that gives high skid resistance at high speeds under both wet and dry conditions and is durable for an acceptable length of time. In order to establish such a configuration, a better understanding of the wear phenomenon is necessary.

The wear of concrete pavement is influenced by the number of wheel passages, properties of concrete and concreting materials, types of tires, pavement roughness, vehicle characteristics, temperature, and weather effects. It should be noted that the effect of studded tires is not considered in this study. Since it is known that wear is accelerated by increased traffic volume, the number of wheel passes would be expected to be a major factor. This is confirmed by prior research by the Council as summarized in Figure 1. (23) The wheels passing over the pavement impart loads to the surface which might result in a micro-scale material loss of polishing (where small pieces of paste or aggregate would be removed) or a macro-scale material loss (where larger pieces of material could break away at zones of high stress). After the pieces break away, new highly stressed zones should develop in the remaining surface configuration and cause new pieces to break away. Because of the complexity of the mechanical interactions and the heterogeneity of concrete a quantitative evaluation may not be possible but even qualitative indications will be of value in identifying the most probable areas of failure.

To investigate the pavement wear mechanism in the presence of grooves, the top pavement surface and the area below the top surface and around the grooves were considered.

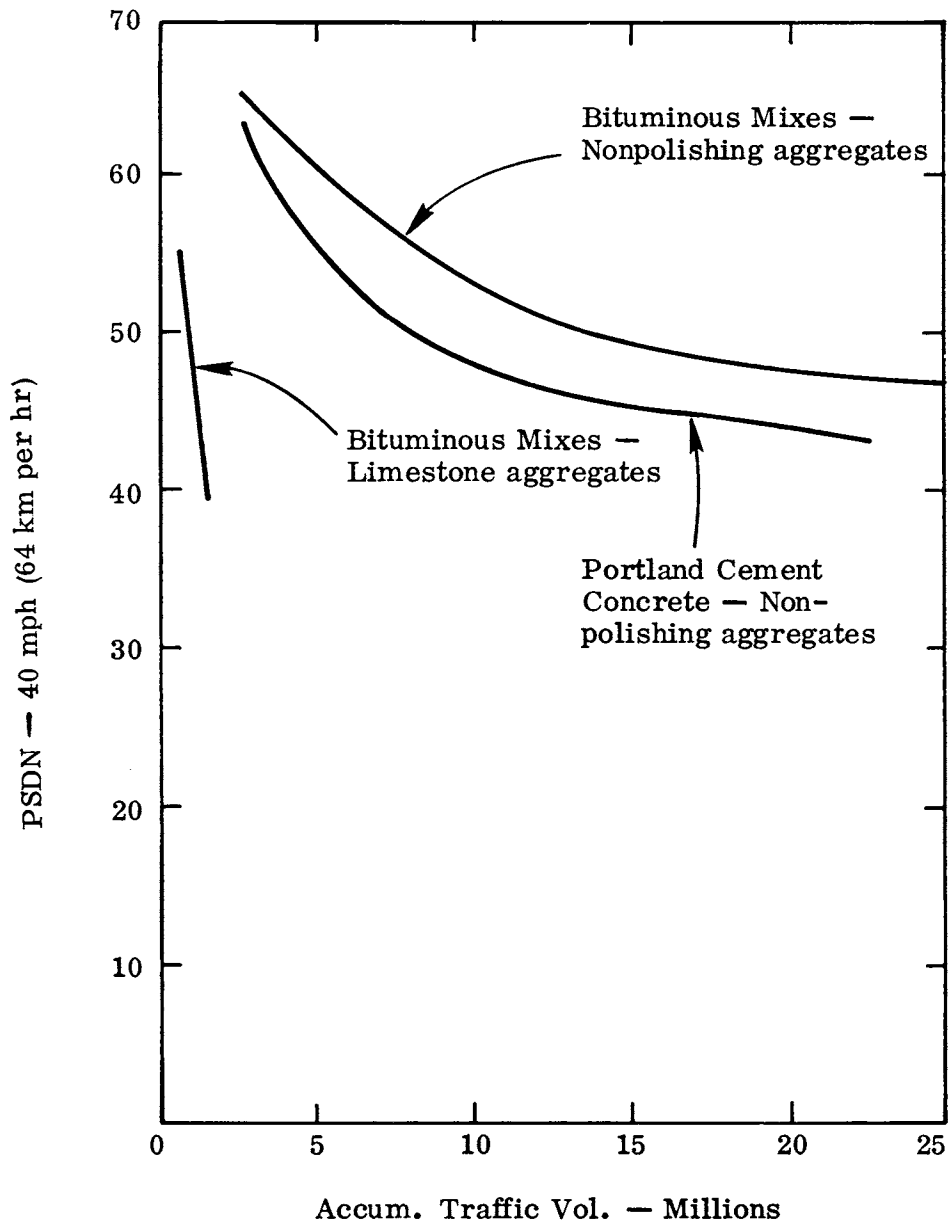


Figure 1. Traffic volume versus stopping distance car skid numbers (PSDN). (From reference number 23.

If the effect of stresses on the wear mechanism can be explained, a durable surface groove configuration, including the geometrics of the surface grooves, the pattern, depth, and width of the grooves, and the spacing between them, can be identified, assuming that the physical roughness and the strength or abrasion resistance of the surface are satisfactory. (24)

#### PURPOSE AND SCOPE

The main objective of this study was to establish the factors that influence the durability of the surface configurations that are used or can be used to provide long lasting and high skid resistance for portland cement concrete pavements. The work consisted of both theoretical and experimental phases within the following scope:

- (1) Concrete cores were extracted from different locations of pavements in service and having coarse textures. Specimens with different levels of wear were obtained.
- (2) The surface and near surface regions of the core samples were studied under a microscope.
- (3) Slabs with various surface textures were fabricated and then subjected to wear under laboratory conditions.
- (4) Resistance of selected textures to freezing and thawing was determined in the presence of deicing chemicals but in the absence of traffic.
- (5) A theoretical approach was developed for calculating the internal stresses around the grooves under a loading which approximates that occurring at the tire-pavement interface in the absence of studded tires.
- (6) The wear observed on the worn surfaces was correlated with the calculated stress distribution in an attempt to establish the pavement wear mechanism.

#### RESEARCH APPROACH

To establish the pavement wear mechanism the top surface of the pavement was investigated experimentally and the area below the top surface and around the grooves was studied theoretically. Lab studies were pursued and concrete slabs having different surface textures were prefabricated and tested on the circular test track of the Maryland Road Commission. After 1,670,000 wheel passes, no appreciable wear was observed. Because of the time required to obtain appreciable

wear as indicated during the tests, concrete cores experiencing various degrees of wear were extracted from actual highways. The specimens included saw-cut grooves (1/8" x 1/8" (3.2mm x 3.2mm) groove) imparted to the worn concrete surfaces and also textures imparted to the fresh concrete pavements by burlap drag and metal tines. The cut grooves and metal tines generate fairly uniform textures, while the burlap drag procedure develops random texture.

Thin sections were prepared from the cores and were studied microscopically to observe the crack development, the loss of material at the surface and the surface texture. Variation in the strength of the paste and its effect on wear were also observed.

The structural behavior of the area below the top surface and around the grooves was investigated using the finite element method. The theoretical analysis involved the determination of internal stresses within the concrete under an assumed surface loading for square, round and triangular configurations.

The experimental results obtained from the samples with saw-cut grooves were correlated with theoretical results derived from the square groove configuration. The geometry of the groove was varied to observe its affect on the internal stresses. Deeper grooves would provide better drainage.

The freezing and thawing durability of the round, square, and triangular grooved surfaces in the presence of deicing chemicals but without traffic was studied. The uniform textures were imparted to a test slab which was put in an outdoor exposure area and subjected to cycles of freezing and thawing in the presence of NaCl.

## EXPERIMENTAL ANALYSIS

### Test Track Studies

Concrete slabs having different uniform and random rough textures were prefabricated and tested in the circular test track. Initially, it was anticipated that noticeable progressive wear of the surfaces could be achieved, and an appreciable decrease in the texture depths could be obtained. The slabs were subjected to 1,670,000 wheel passes but no discernible wear was observed. This indicated that to obtain a significant decrease in texture depth utilizing the circular track might be possible only under a very large number of wheel passes. Because of the time limitations of the project and feasibility of occupying the track for a long period of time the experimental effort was redirected to the study of concrete cores extracted from the pavements in service. The procedure and results from the test track are included in the Appendix.

Field Concrete CoresSampling

Since no appreciable wear was observed on the test slabs and no facilities were available for fast, large-scale wear, samples with varying degrees of wear were taken from existing highways. Nine cores were extracted from I-95 in Henrico County, six from I-64 in New Kent County, and four from I-64 in Albemarle County, using a truck-mounted drilling rig. In Henrico County, at the intersection of I-95 and Route 301, six of the samples were taken from the longitudinally grooved section and the other three from the transversely grooved section. The longitudinal grooves were originally 1/8" (3.2mm) deep and wide with 3/4" (19.0mm) spacing. The transverse grooves were also 1/8" (3.2mm) deep and wide but were spaced 1" (25.4mm) apart.

This portion of I-95 was completed in 1962. Later, in May 1969, it was grooved to improve the frictional properties. Because of the high and increasing traffic volume, the grooves were losing their depth or even disappearing. The samples were taken from in and out of the wheel path in the southbound traffic lane to obtain unworn and moderately and heavily worn surfaces. The fine aggregate used in the pavement was quartz river sand obtained from the Mattaponi Sand and Gravel, Aylett, Virginia. The coarse aggregate was granite (fine to medium grained gneiss) produced by General Crushed Stone, Verdon, Va. The paving mixture, class A-3 concrete, as required by the Virginia Department of Highways are summarized in Table 1. (25)

Table 1

The Requirements for Virginia Department of Highways Class A-3 Paving Mixture

Design Minimum Laboratory Compressive Strength at 28 Days: 3,000 psi

Aggregate Size Number	(3) 57
Minimum Grade Aggregate	A
Minimum Cement Content	6 bags/cu. yd. (335.6 kg/cu. m.)
Maximum Water-Cement Ratio	.49
Slump	0-3 in. (0-76mm)
Air Content	6 ± 2 percent

On the portion of I-64 in Albemarle County near Charlottesville two samples were taken from the wheelpath and two outside the wheelpath in the westbound traffic lane. This pavement was completed in December 1970, and the fresh concrete was finished by multiple burlap drag. The fine aggregate was obtained from Southern Materials Co., Richmond, Va. The coarse aggregate was

biotite granite gneiss produced by Superior Stone Co., Red Hill, Virginia, the same aggregate as that used in the laboratory specimens. In 1973, appreciable wear of the surface was observed in the wheel paths.

The portion of I-64 in New Kent County was completed in late 1972. During construction deep grooves were imparted to the surface with metal tines. Tine spacings of 3/4" (19.0mm), 1/2" (12.7mm), and 1/4" (6.4mm) were used. This pavement had not experienced much traffic at the time cores were extracted so significant wear had not taken place. Two samples for each spacing were obtained from the right wheelpath of the traffic lane. The aggregates were siliceous sand and gravel. The gravel coarse aggregates were obtained from West Brothers Sand and Gravel, Strath Road, Richmond, Va., and the fine aggregates from J. R. Parker, Providence Forge, Va.

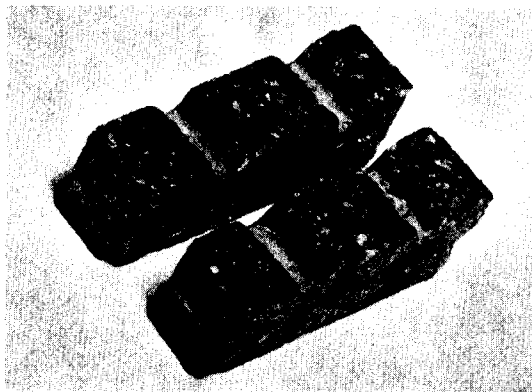
#### Preparation and Investigation of Thin Sections

To observe the progress of wear, thin sections were prepared from the cores and studied under a microscope. (26,27) This examination made possible a qualitative description of the crack development around the grooves, the existing surface texture, the orientation and the types of aggregates and the loss of material at the surface.

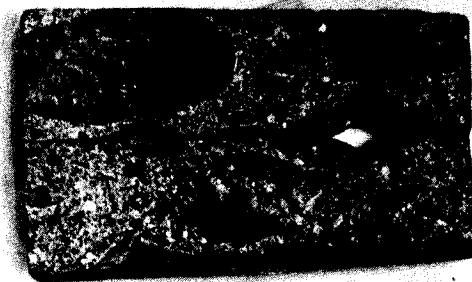
Thin sections were obtained from the concrete cores by cutting chips about 1/4" (6.4mm) wide, 1 3/4" (44.4mm) long, and 1/2" (12.7mm) deep vertically, both perpendicular and parallel to the groove direction at the surface. Two chips were mounted on the same slide with their top surface edges facing each other and running the length of the slide. Then the chips were cut and ground to the desired thickness and a cover slip was cemented on as a protection. The preparation of thin sections from pavement core surfaces is shown in Figure 2.

The thin sections were 50 $\mu$ m thick. The maximum thickness of petrographic thin sections used for other purposes is usually 30 $\mu$ m. The 50 $\mu$ m thickness was selected as a compromise between good observation conditions and physical completeness of the specimens. The thinner the section the greater the clarity, the sharper the focus, and the less the diffusion of the light. However, with thicker sections there is a lesser danger of losing the lightly attached aggregates and paste near cracks during preparation.

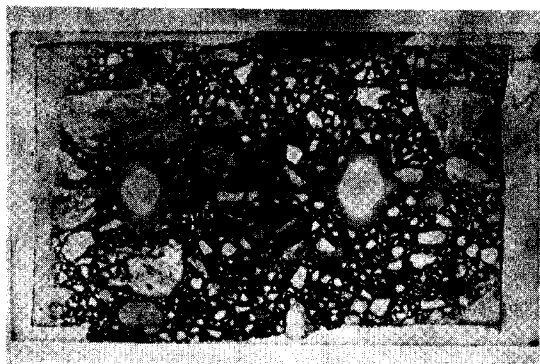
The plane of the cracks is randomly oriented and is irregular throughout the material in three dimensions. In the case of microcracks traveling in directions other than perpendicular to the plane of the thin section, the presence of paste or aggregate beside the crack in the path of the light might obscure the passage of light. This may appear as a discontinuity along the path of the crack in the plane of the thin section. Of course, certain discontinuities might be real because of a sub-microscopic granulation of material filling the crack space or because of a partial healing of the crack by subsequent hydration of cement material.



Chips cut at the surface of  
the sample



Chips mounted on a glass  
slide



A plan view

Figure 2. Thin section preparation of pavement core surfaces.

Results from petrographic observations are of necessity qualitative but considerable insight into the pavement wear process can be gained from the typical results shown in Figures 3-6.

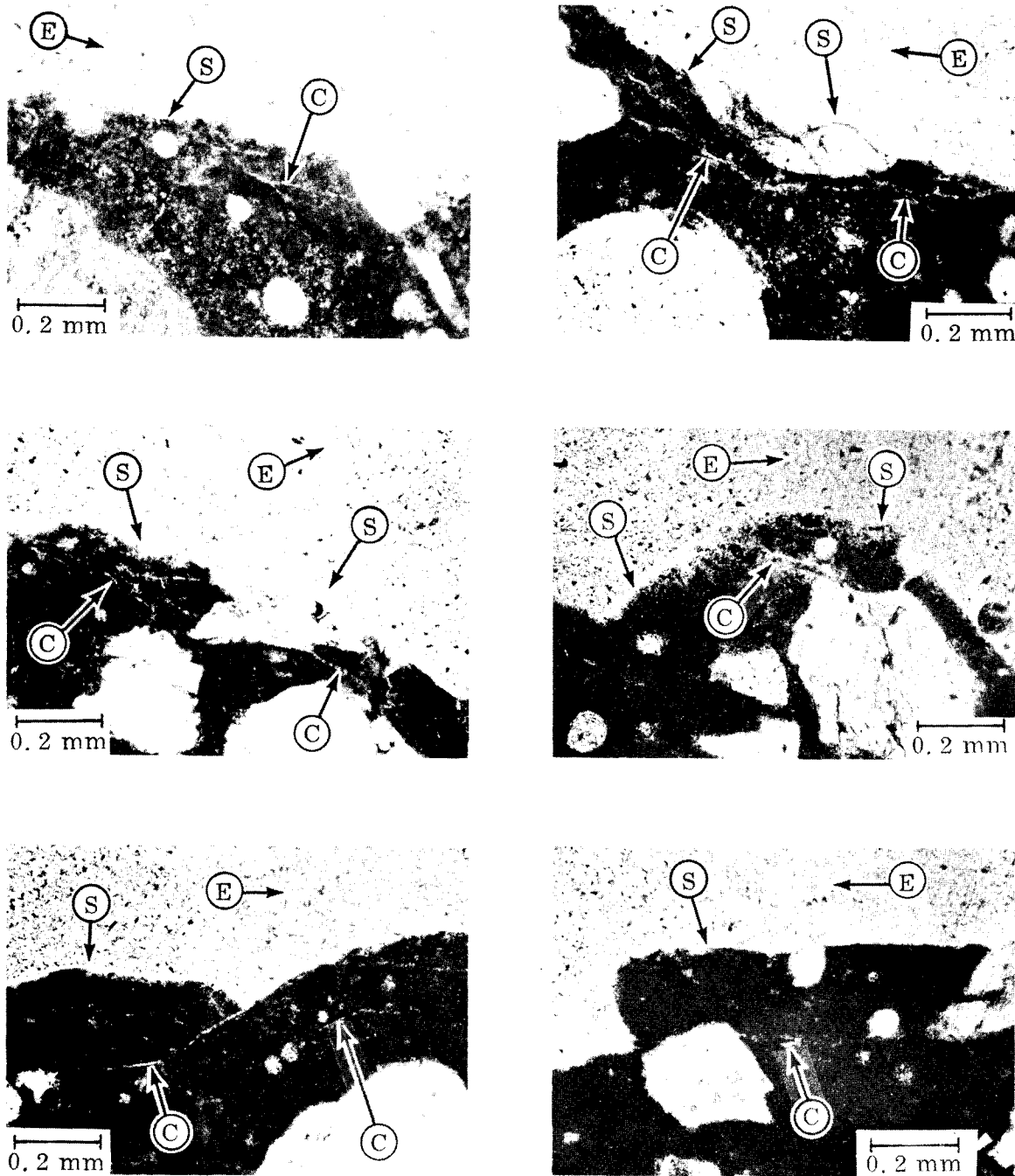
The thin sections obtained from I-95 showed a strong paste with a low water-cement ratio and air content. Most of the microcracks present in the paste occurred about 0.2mm below the surface. As shown in Figures 3 and 4, these cracks propagated parallel to the surface until the material enclosed became loose and was displaced. These flaking type cracks were considered to result mainly from the repetitive loads imparted by the traffic. Environmental effects cause cracks with different characteristics. Freeze and thaw cracks are deeper in the material and tend to be horizontal, usually about 2mm below the surface. Shrinkage cracks have a more random distribution and often concentrate at the paste aggregate interface. The association of cracking with the interface and/or the progression of the cracks through rather than around the aggregates depend upon material properties and that age at which the strain occurs. Hardened past has an elastic modulus of 1 to 4 x 10<sup>6</sup> lb/in<sup>2</sup> (7 to 28 GPa); whereas that of aggregates is 5 to 10 x 10<sup>6</sup> lb. in<sup>2</sup> (34 to 69 GPa). (28) This difference could cause cracks at the interface of the aggregates.

In the strong paste, besides flaking, other types of cracks were seen, some at the paste aggregate interface, and some perpendicular to the surface and penetrating deep into the paste (possibly predetermined by an air void as shown in Figure 5) and some caused by crushing of the paste as shown in Figure 6.

In figure 5, crack number five looks as if it is discontinuous. A similar trend was observed in other cracks as well. However, as explained previously it is hard to determine the path and nature of the cracks.

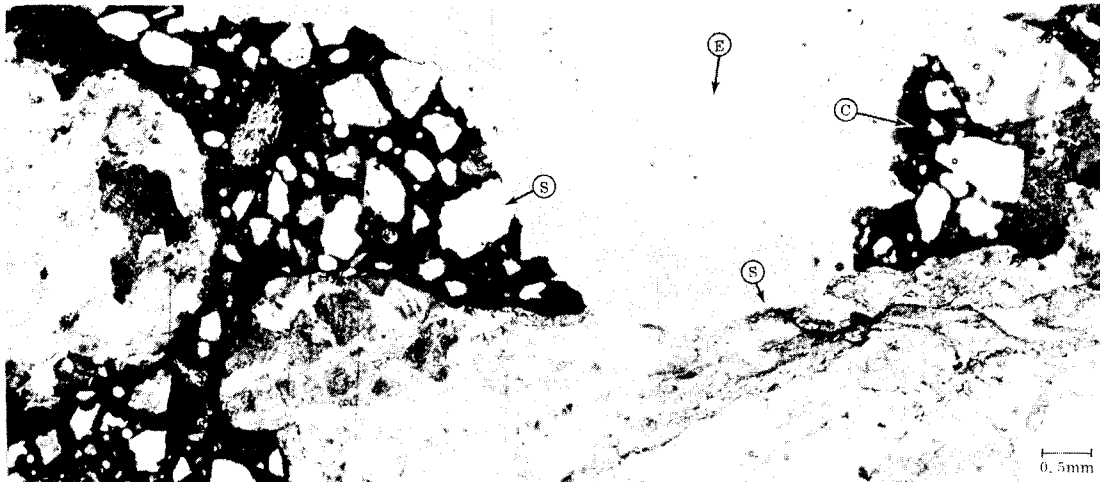
In the less worn specimens where an appreciable groove depth was present more cracks were seen in the areas between the grooves than were seen in the highly worn specimens. In both cases the cracks were distributed evenly. This even distribution suggested that the fewer number of cracks in the worn grooved pavements was due mainly to the presence of tougher paste with fewer air voids away from the top surface. There were hardly any cracks at the bottom of the grooves. At the shoulders of the grooves, the locations where the groove meets the upper surface, flaking type cracks existed as shown in Figure 3. The shoulders of the grooves wore faster than the top surface, most probably because of a lack of restraint on one side and because of higher surface pressures imparted to them under a flexible tire. The tire might stretch and exert higher pressures at the edges. As the wear progressed the grooves widened until a level was reached where the groove disappeared. This is illustrated in Figure 7.

Both the longitudinal and the transverse grooves seemed to indicate the same trend as far as wear was concerned. In a few of the deep grooves a vertical crack near the groove was noticed as shown in Figure 8. Due to the limited quantity of samples studied, the existence of this crack was not attributed to any specific cause.



- Ⓔ Epoxy potting resin
- Ⓕ Surface profile
- Ⓖ Crack

Figure 3. Photomicrographs of thin sections showing surface cracks that cause flaking.



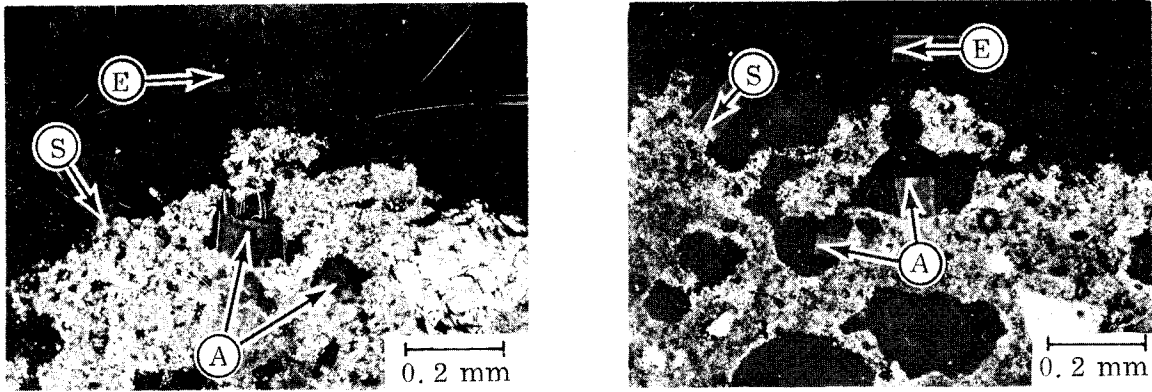
- Ⓔ Epoxy potting resin
- Ⓕ Surface profile
- Ⓖ Crack

Figure 4. A groove cut from I-95 is pictured in thin section. The bottom of the groove is round because of the saw cut. The arrow in the top picture points out a flaking crack enlarged in the picture at the bottom.



- (E) Epoxy potting resin
- (S) Surface profile

Figure 5. Cracks other than those that cause flaking in the near surface (1) and (2) show cracks perpendicular to the surface which penetrate into the material. Possibly the cracks will travel at the interface of the fine aggregate and the paste and dislodge the surface material. (3), (4), and (5) show cracks in the paste. (6) shows a preexisting crack in the coarse aggregate that propagates at the interface and into the paste. (7), (1), (2) and (5) show the influence of air voids on cracks.



- (A) Air void
- (E) Epoxy potting resin
- (S) Surface profile

Figure 6. Photomicrographs showing the crushing of the paste predetermined by an air void.

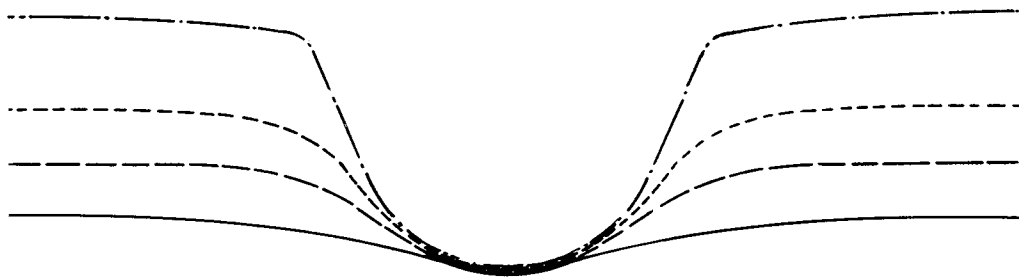
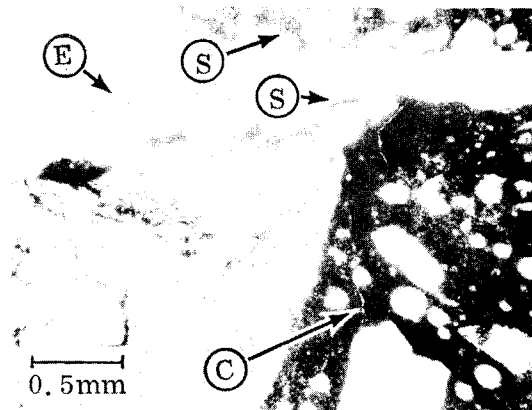


Figure 7. Progressive wear modeled after the specimens obtained from the grooved section of I-95 at intersection with Route 301. The bottom of the grooves is considered as datum.



- Ⓔ Epoxy potting resin
- Ⓕ Surface profile
- Ⓖ Crack

Figure 8. In a few deep grooves a vertical crack near the groove was observed.

The samples prepared from the cores taken on I-64 in Albemarle County showed the presence of a weak paste at the very top surface, less than 0.5mm deep. Underneath this thin weak layer of paste, the presence of more aggregate and fewer air voids provided a stronger concrete matrix. The weak paste was the result of a high water-cement ratio, bleed channels, and a high percentage of air voids. It disintegrated into small chunks rather than flaking as a result of the crushing of the paste, initiated by the presence of the air voids and asperities as shown in Figure 6. The fine aggregate was river sand with planes of weakness. Very few coarse aggregate particles (biotite granite gneiss) were exposed. These particles also had planes of weakness. The brittle character of the aggregates caused chips to come off, and provided for the maintenance of a good microtexture. This section of I-64 was textured by burlap drag. The path under the wheels was worn but retained its microtexture.

In the stretch of pavement on I-64 in New Kent County, the paste examined showed characteristics similar to those of the paste on I-64 in Ablemarle County. It had a high water-cement ratio at the top surface. The quality of concrete beneath this layer was better. Mainly crushing of the paste occurred. The aggregates used were sand and gravel obtained from the same source. Some were toughened by metamorphosis, so they adhered to each other very well. Some were friable.

This portion of I-64 had been opened to traffic recently. On the surface a very good microtexture, a large number of asperities and no polishing were observed, as seen in Figure 9. At the bottom of the grooves deposits of mortar were noticed (Figure 9). These might be due to the finishing operations when loose surface mortar might have been carried to the bottom of the groove.

When the groove spacings were large, more fine aggregates were exposed at the surface, and the coarse aggregate was closer to the surface. The more closely spaced tines appeared to have pushed the coarse aggregate down and left mainly mortar in the area between the grooves.

The weak layer of paste seen in both portions of I-64 might be attributable to the texturing methods on fresh concrete. The burlap drag or the metal tine might cause some disturbance that would result in the accumulation of water in the near surface area. Another possibility is that during mixing a weak layer of paste with a high water-cement ratio might form at the surface because of bleeding.

The top surface of a fresh mix might be weak regardless of the quality of the mix. As this weak surface wears off, the concrete exposed can yield high and long lasting skid resistance, provided the mix is of good quality.

The paste at the surface was observed to contain more  $\text{CaCO}_3$  than the paste at the bottom of the grooves. The carbonation of cement paste produces a hard surface layer in which healing cannot take place. This layer might well be considered more brittle when compared to the partially hydrated, uncarbonated paste below.

The top surface of the grooved, rough textured pavements showed more carbonation than the bottom of the grooves. This may be due to the fact that carbonation mainly occurs at 50% R. H. (relative humidity) and is a slow process for zero and 100% R. H. Fifty percent R. H. is expected to occur at the top surface rather than at the bottom of the grooves, which act as water channels. The samples from the new section of I-64 showed less carbonation than the others since carbonation is a time-consuming phenomenon.

The texture should be deep enough so that when the top weak surface wears away an appreciably rough texture can be maintained. At some locations on I-64 west of Charlottesville the original texture was not too deep and the microtexture had disappeared. On I-64 in New Kent County, even when the top surface wears away there will still be some rough texture to provide the necessary frictional properties.



- Ⓔ Epoxy potting resin
- Ⓕ Surface profile

Figure 9. New section of I-64 east of Bottoms Bridge showed good microtexture, large number of asperities at the top surface and deposits of mortar at the bottom of the grooves.

### Freezing and Thawing Durability of Uniform Shapes

To investigate the freezing and thawing durability of the round, square, and triangular grooved surfaces in the presence of deicing chemicals but without traffic, one test slab was prepared as shown in Figure 10. The three uniform textures were imparted to the surface of the slab side by side. A class A-3 mixture with Type II cement was used and a 6% air content was obtained. The slab was put in an outdoor exposure area and subjected to cycles of freezing and thawing in the presence of NaCl.

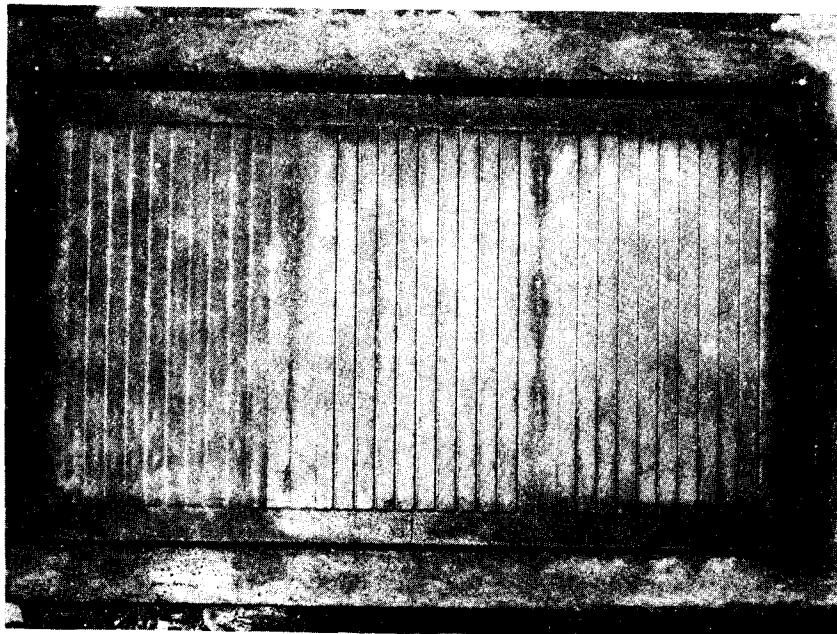
In each cycle a measured volume of water was poured on the slab and allowed to freeze. NaCl in the amount of 2% of the weight of that water was placed on the slab. It was then allowed to thaw and freeze again. After the next thaw, the surface was flushed clean and another cycle began. This program resulted in 50 cycles of freezing and thawing, half in the presence of deicing salt and half in plain water.

The specimen showed scaling that would be classified by ASTM Method C 672 by the rating 1, the condition being very slight scaling. (29) After 50 cycles of freezing and thawing, it was not possible to distinguish differences in the durability of various groove configurations as shown in Figure 10. In ASTM Method C 672, it is stated that 50 cycles may be sufficient to evaluate a surface. In comparative tests if differences are not developed after 50 cycles, it is recommended that additional cycles be run. However, in this project, because of the limited time involved, the specimen was subjected to only 50 cycles of freezing and thawing. These results confirm that the durability of properly proportioned and finished concrete, even with severe textures, is adequate in the absence of traffic.

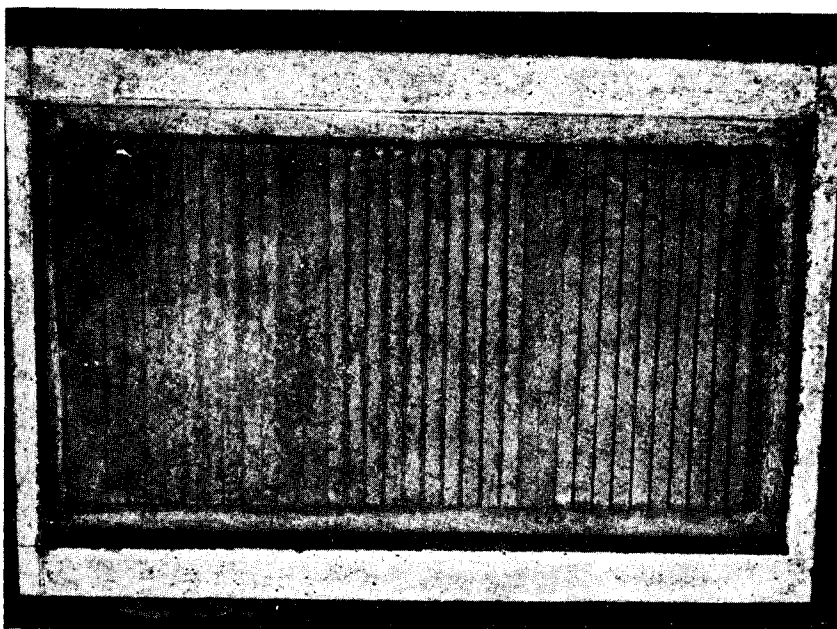
## THEORETICAL ANALYSIS

### Surface Configurations and Material Properties

To investigate the wear mechanism of the grooved pavements from the standpoint of surface stresses, a theoretical analysis was performed. Most theoretical studies require idealization of the parameters involved (such as loads, surface configurations, and materials), so a limited number of different uniform groove patterns with the same spacing and texture depth were studied. These patterns are shown in Figure 11. The dimensions of the square groove were chosen based upon indications from the published literature describing cases in which this pattern is currently in use and is performing satisfactorily. (15, 16)



Before exposure to weathering.



After exposure to 50 cycles of weathering.

Figure 10. Freeze and thaw specimen with round, square and triangular grooved surfaces.

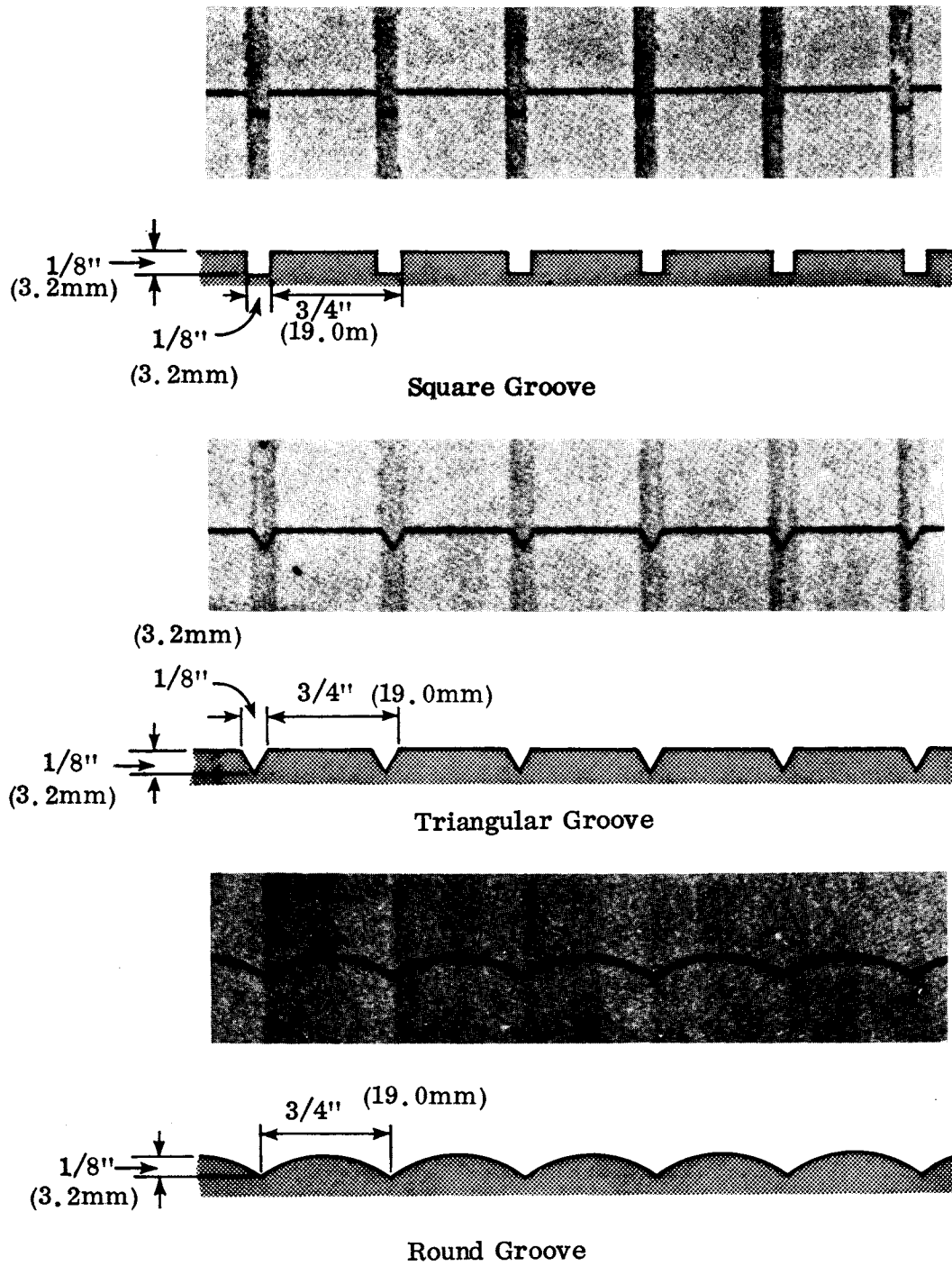


Figure 11. Uniform groove patterns chosen for the theoretical investigation of the wear mechanism.

Concrete is a nonhomogeneous material. In the theoretical study, however, it was assumed to be homogeneous, isotropic, and elastic. The elastic modulus was calculated using the formula: (30)

$$E = 33w^{3/2} (f'_c)^{1/2}$$

Where  $f'_c$  is the design compressive strength in psi,  $w$  is the unit weight of hardened concrete in pcf, and  $E$  is the elastic modulus in psi. For paving concrete used by the Virginia Department of Highways,  $f'_c$  is assumed to be 3,000 psi (20.7 MPa). The unit weight was taken as 145 pcf (2320 kg per cu. m). These values give  $E$  a value of  $3.2 \times 10^6$  psi (22.1 GPa). In order to supply the second necessary material property for the analysis, Poisson's ratio,  $\nu$  was approximated as 0.17. The tensile strength of concrete was assumed to be 300 psi (2.1 MPa), 10% of its compressive strength.

### Surface Loads

A vehicle transmits loads to the pavement through the tires; thus the tires support the vertical load and develop traction forces to propel, stop or steer the vehicle. The forces generated at the tire-pavement interface can be divided into two components; the normal and the tangential. The tangential (frictional) stresses at the surface can be resolved into two parts, one along the direction of travel and the other in the transverse direction.

The distribution of the vertical tire contact pressure depends primarily on the tire inflation pressure. Other parameters that affect the surface pressure include structural and operating characteristics of the tire. Vehicles with a wide range of weights operate on the highways, but the tire contact pressure is not significantly affected by an increase in static loads. The differences in weight among the various vehicles on the highways are accommodated by an increase in the tire contact area incident upon an increase in load, which allows the tire contact pressure to remain virtually unchanged. At the Army Mobility Research Center in Vicksburg, vertical contact pressures on rigid surfaces beneath several pneumatic tires with smooth threads were measured. (31) It was found that for a 11.00-20, 12PR smooth tire under a 3,000 lb. (1.361 Mg) load (intermediate between a truck and a passenger car wheel load) at a 30 psi (207 kPa) inflation pressure, the contact pressure along a transverse centerline may vary from 0 to 120 psi (0 to 827 kPa) at the ends. On both sides of the centerline it drops to 40 psi (276 kPa) for most of the width. It would appear, then, that a groove in the pavement near the edge of the contact area is loaded by 100 psi (689 kPa) average vertical pressure. This was assumed to be the case for the purpose of this study.

As far as the lateral shear forces are concerned, limited data were available to the author. In NBS Monograph 122, 1971, Mechanics of Pneumatic Tires, it is stated that the exact distribution of the lateral shear stresses is not well understood, even for a stationary tire. (32) Furthermore, different types of tires would create different lateral shear forces. A figure given in the same book shows

the stress distribution across the width of an aircraft tire reaching a maximum shear stress of 75 psi (517 KPa). In this study, for a rolling tire, a lateral shear force of 25 psi (172 KPa) was assumed. This value was determined on the assumption that the lateral friction force would be 25% of the normal force for a rolling tire. Initially, internal stresses in the pavement were calculated using the above value. A second series of computations with the shear stresses increased to 75% of the normal pressure was made in order to determine the effect on internal stresses from extreme conditions such as cornering or braking.

In the case of round grooves two different contact areas (which are considered to be limiting cases) were studied. In one case, a test slab having the round groove was loaded by a stationary smooth tire with a 1,000 lb. (454 kg) loading and the contact surface was measured. In the other case, the polished surface area was determined for a test slab with round grooves which had been subjected to wear on the test track. In order to accommodate the diminished contact area of the rounded grooves under constant loading the surface pressure was increased proportionately in the theoretical analysis to 125 and 200 psi (0.862 and 1.379 MPa) normal pressure for the two different cases. First 25% then 75% of these normal pressures were taken as shear loads.

#### Internal Stress Evaluation

The grooves had sharp corners where stress concentrations would be expected to occur. (33, 34) At these points, a rapid variation of stress is also expected. Stress values can be evaluated for solid bodies of varying geometries using mathematical methods. However, as the geometric conditions become more complex, the analytical methods lead to differential equations that are very difficult to solve. (35) In such cases, numerical methods are normally used. Numerical methods give approximate, but satisfactory, values of the desired quantities at a finite number of points. (36)

Experimental procedures have also been used successfully whenever the analytical solutions have been impractical or complicated. Some of the experimental methods used are: photoelasticity, elastic membrane, electric analogy, strain gage, brittle coating, brittle material, ductile material, rubber model, and the repeated stress techniques. (35, 37)

All potential approaches having been considered, the different groove patterns in this investigation were analyzed using the finite element method because of complex geometric conditions at the grooves.

The concrete surface was investigated as a two-dimensional problem rather than the actual three-dimensional one. This was done to simplify the problem. The capacity of the available computer is limited and the use of three-dimensional elements occupies a large memory space. The section of pavement perpendicular to the longitudinal grooves was analyzed. This section is the critical one since it includes the complex boundaries.

The two-dimensional model is treated as a plane strain problem. This approach assumes that the predominant strains occur in a plane and that the stresses in the other direction are neglected because of the small Poisson's ratio for concrete.

### Finite Element Method

The fundamental concept in the finite element technique is that a structure may be considered as an assemblage of individual elements interconnected at a finite number of joints or nodal points. (38, 39, 40, 41, 42) For example, the two-dimensional elements interconnected at nodal points around the half grooves investigated in this study are shown in Figure 12.

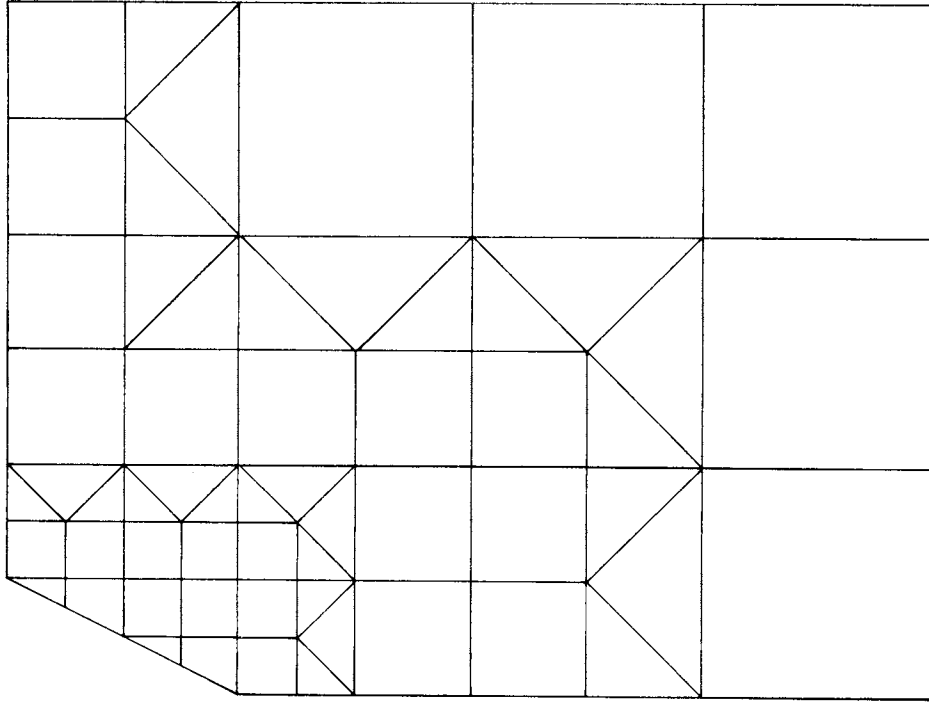
The finite element analysis involves three basic steps: (41)

- (1) Structural idealization,
- (2) derivation of the element properties, and
- (3) structural analysis of the element assemblage.

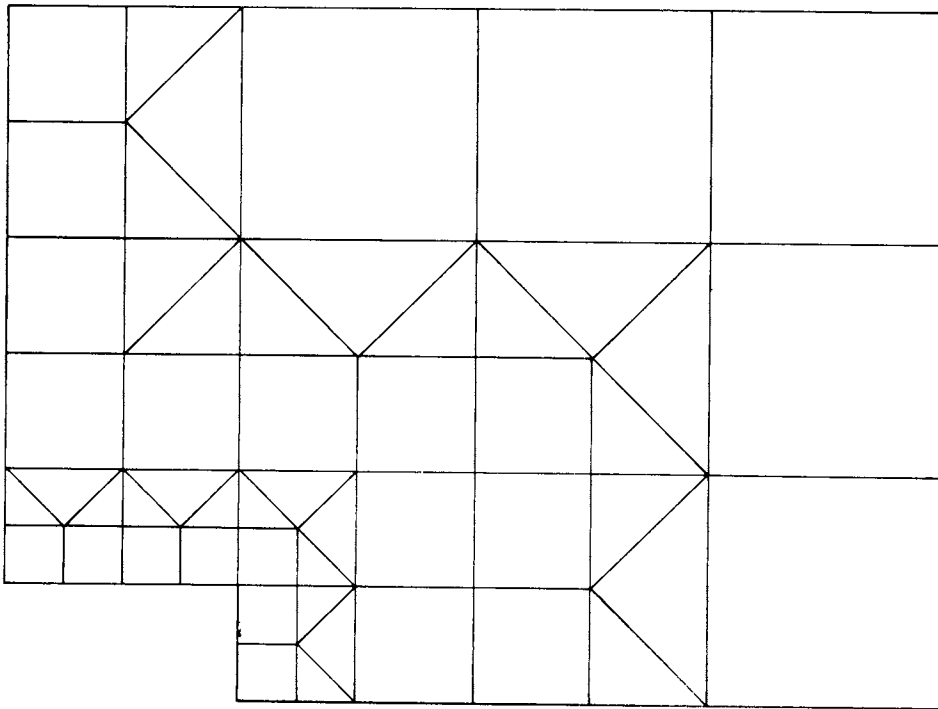
The structural idealization is simply the discretization of the system. Discretization means the subdivision of a given system into an equivalent system of finite elements. Then the properties of the chosen element are evaluated. This evaluation consists of determining the stiffness or the flexibility of the element, which relates the nodal forces to the nodal displacements. The individual element properties are combined to obtain the overall stiffness, or the flexibility matrix of the system. Afterwards, the computation of stress and deflections for a given loading condition is a standard structural problem and the following three basic principles should be satisfied: (41, 43)

- (1) Equilibrium of the internal element forces at each node with the externally applied nodal forces,
- (2) compatibility of the element deformations at the nodes, and
- (3) force-deflection relationship for each element according to the geometry and the material properties.

The unknown quantities in the analysis may be the nodal displacements, the nodal internal forces, or both. The corresponding methods of analysis are known as the displacement (stiffness) method, the force (flexibility method), or the mixed method. (42) For each element, the relation between the displacements and the internal forces of each node is formulated according to the theory of elasticity. The equations obtained are very conveniently expressed in matrix notation. The element matrices are assembled to represent the complete structural system. The matrix formulation of a structural system yields simultaneous algebraic equations suitable for automatic computation. In fact, for a large number of elements it would be impractical, if not impossible, to handle the volume of data manually.



Triangular Groove



Square Groove

Figure 12. Half the groove and the surrounding mesh distribution formed by the two dimensional elements.



In the force method of analysis for an indeterminate structure, there are several alternatives in the choice of the redundants. (The redundants are the forces in excess of the number needed to obtain a statically determinate structure.) Each choice of redundancy will influence the nature and the amount of the computation necessary.

In the stiffness method the unknown quantities are the joint displacements. (The joints of a structure subjected to load will experience displacements unless they are restrained.) The unknown joint displacements will dictate the degree of indeterminacy and there is no question about their selection. Thus, the stiffness method can be readily standardized and does not require engineering decisions during the computations. (44, 45) Hence for computer use the stiffness method is more desirable, thus, in the finite element technique the displacement method is usually employed. There is a lack of a generalized and systematic flexibility method. (36)

### ELAS Program

In this study a computer program called ELAS75 was used to determine the stresses around the grooves of the top surface, subjected to an assumed loading condition. ELAS75 is an improved FORTRAN IV version of the ELAS program, (46) a digital computer program for solving the linear equilibrium problems of one-, two-, and three-dimensional systems. It has been used in aerospace and related industries since 1966. ELAS75 has been adapted to the University of Virginia computer system using UPDATE, a system program that enables the creation, manipulation, and maintenance of library files for the SCOPE operating system. ELAS75 consists of a main program and about 100 subroutines. \* To minimize the core memory area for the instructions, the program is overlaid into four basic links. The first link reads, stores, and checks the input data. The second link generates the governing equations of the problem by generating and assembling element stiffness and load matrices. The third link solves for the deflections, and the fourth link obtains the stresses. The program consists of the displacement method of analysis and the finite element method. The availability of one-, two-, and three-dimensional elements provides for the solution of almost any structure. The deflections between mesh points are assumed to be linear. This assumption ensures the monotonic convergence of deflections from the stiffer side with decreasing mesh size. (46)

The computer program used gives the stress values at the centroid of the element. To determine the number of nodes necessary for good results, a coarse and then finer mesh were analyzed. Elements of the refined mesh were chosen such that their centroids coincided with the centroids of the elements of the coarser mesh. The degree of convergence of displacement and stress values at the common points dictated whether or not still finer meshes were necessary.

---

\* The ELAS75 computer program listing is complex and long. Therefore, it is not attached to this report but is in the Research Council files.

Computations, Results, and Conclusions

In the pavement cross section, the highly stressed regions would be those at the top surface and around the grooves beneath the contact area. Because of practical limitations, such as the capacity of the available CDC 6400 computer, only a small portion of the top surface could be studied. Therefore, as shown in Figure 13, a part of the surface with one groove was considered and it was called the "small system". The rest of the pavement cross section influenced by the surface loading was called the "total system". The mesh distribution of half the small system with different groove patterns is shown in Figure 12. The depth of the small system was taken as 1/2" (12.7mm), four times the actual maximum groove depth, so that all the desired stress distribution around the groove could be included. The total system was assembled from elements which became smaller towards the top surface, especially under the surface loading. The mesh divisions were made so that the boundaries and some nodes of the small system coincided with those of the total system. The small groove analyzed is located in the top center portion of the total structure. The boundary conditions of the small system were obtained from the corresponding displacements at the common nodal points of the total system.

It was necessary to choose the dimensions of the total system. If a body is loaded at a surface, a part of the body beneath the surface would be affected. The stresses would decrease as the depth increased. A point would be reached where the stress components would reach only a small percentage of the contact pressure and could be neglected. In the total system this depth would be well below the depth of the concrete pavement, which is usually 8" (203mm) or 9" (229mm). Below the pavement is the subbase, a layer with physical properties that are quite variable and hard to specify. In addition, the displacements and friction forces at the interface between the pavement and subbase are difficult to predict. Because of these complications, the total system was assumed to be of one material. Later as a check, the layer below 9" (229mm) of concrete was treated as a different material having an elastic modulus of 10% of that of concrete. Only a small variation of stresses was observed at the top surface and around the grooves under the tire loading. Based on Boussinesq's equation, which considers that the material is elastic, homogeneous, and isotropic, the depth of the total system was assumed to be 20" (508mm), beyond which the effect of the surface loading was negligible. (47) The width of this system was calculated to be 46 3/4" (1187mm) based on the 45° stress distribution approximation. This approximation assumes that at each depth the vertical stress is distributed on an area bounded by lines originating at the end of the loaded area and descending at an inclination of 45°.

The boundary conditions on the total system were chosen so that no vertical displacement at the bottom and no horizontal displacements at the far ends were permitted. The concrete on both sides of the total system would provide some restraint. However, some lateral movement at the ends would be expected. Therefore, another run of the same system was made with no prescribed boundary condition at both far ends. This assumption had negligible effects on the stresses at the center of the system where the small system was located.

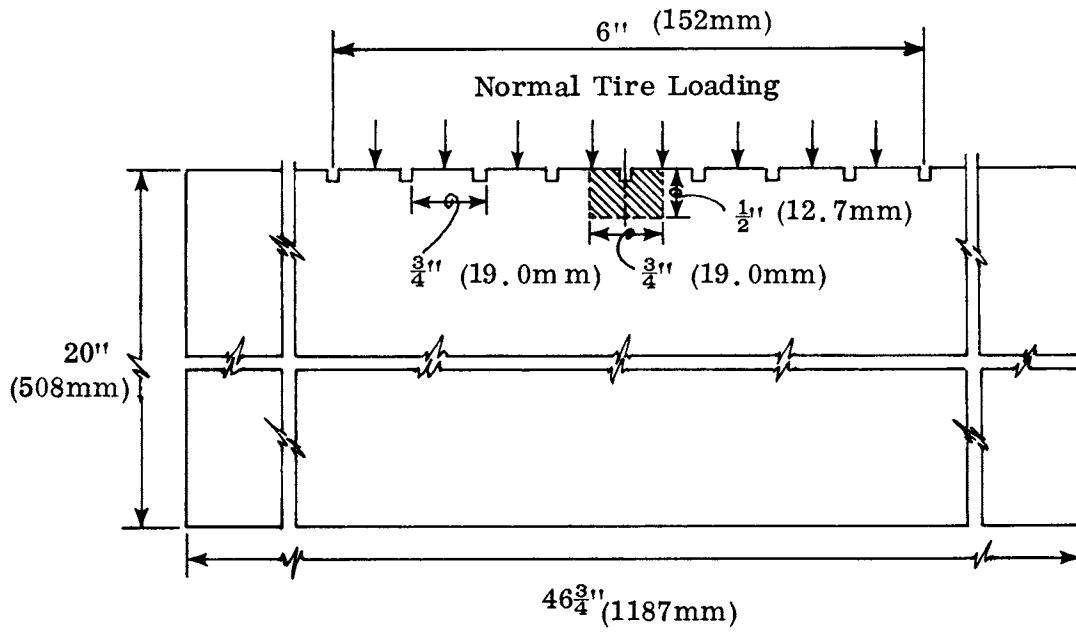


Figure 13. Loaded surface and the resulting area of influence constituted the large model "total system". The shaded portion with one groove represented the "small system".

It should be noted that in the theoretical analysis a constant average elastic modulus,  $E$ , was used for concrete. However, the constituents of concrete themselves have different  $E$  values. The size of the finite elements used in the complete system may be small enough in some cases to approach the dimensions of the constituents of the concrete. However, because of the heterogeneity of concrete, it is not possible to pursue an analysis which will be general and also include the different  $E$  values of the ingredients of concrete.

The four possible loading conditions shown in Figure 14 were applied to the single groove. The necessary boundary conditions were obtained from the total system under tire loadings, shown in Figure 15.

In the analysis, principles of symmetry and antisymmetry were used. This enabled the computation of the displacements and stresses in the complete system by considering only half of the system, divided through the centerline, as shown in Figure 16. The symmetry principle requires only the deformation within the plane of symmetry be specified. Conversely, the antisymmetry principle states that no deformation take place within the plane of symmetry.

When the stress or displacement values for one side of the system are determined, those for the other side can readily be obtained, depending on the symmetry or the antisymmetry conditions. For the stress components the following relations hold.

Primes denote the other half of the body:

$$\text{Symmetry; } \sigma_x = \sigma_x', \quad \sigma_y = \sigma_y', \quad \tau = -\tau'$$

$$\sigma_{1,2} = \sigma_{1,2}', \quad \tau_1 = \tau_1'$$

$$\text{Antisymmetry; } \sigma_x = -\sigma_x', \quad \sigma_y = -\sigma_y', \quad \tau = \tau'$$

$$\sigma_1 = -\sigma_2', \quad \sigma_2 = -\sigma_1', \quad \tau_1 = \tau_1'$$

where  $\sigma_x$  and  $\sigma_y$  are normal stresses  
in  $x$  and  $y$  directions respectively

$\sigma_1$  and  $\sigma_2$  are maximum and minimum principal normal stresses respectively

$\tau$  is the shear stress

$\tau_1$  is the principal shear stress

For the 100 psi (689 kPa) normal and 25 psi (172 kPa) shear loading, the internal stresses in the concrete were well below levels sufficient to cause direct failure in concrete. In Figure 17, stress contours are plotted which show the distribution of principal stresses for type (a) loading (Figure 14), which along with type (c) gave overall high tensile stresses compared to the other types of loading.

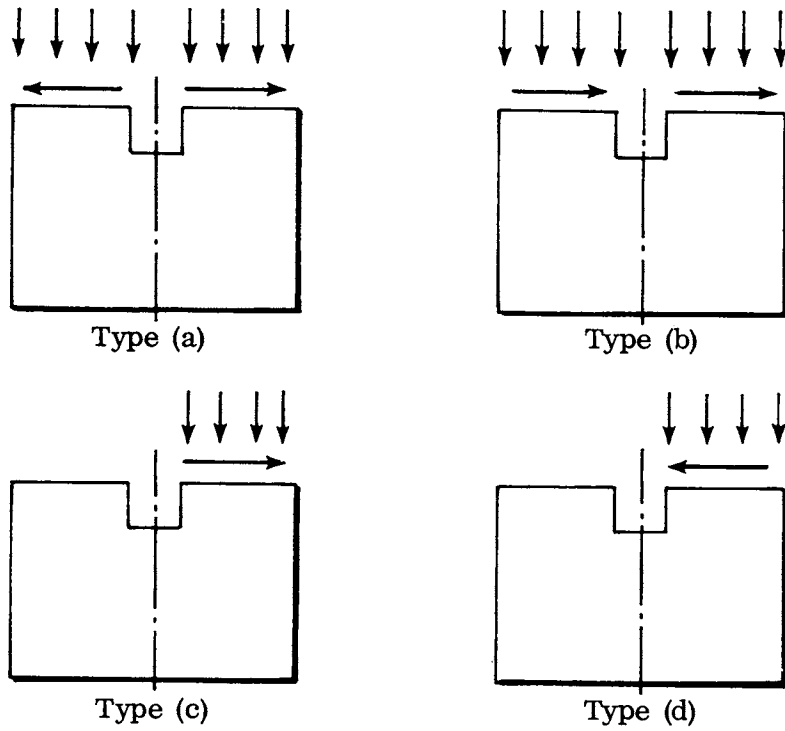


Figure 14. Different types of loading on a groove representing possible extreme cases and different modes of travel such as type (a) would occur along a straight road whereas type (b) would occur around the curves.

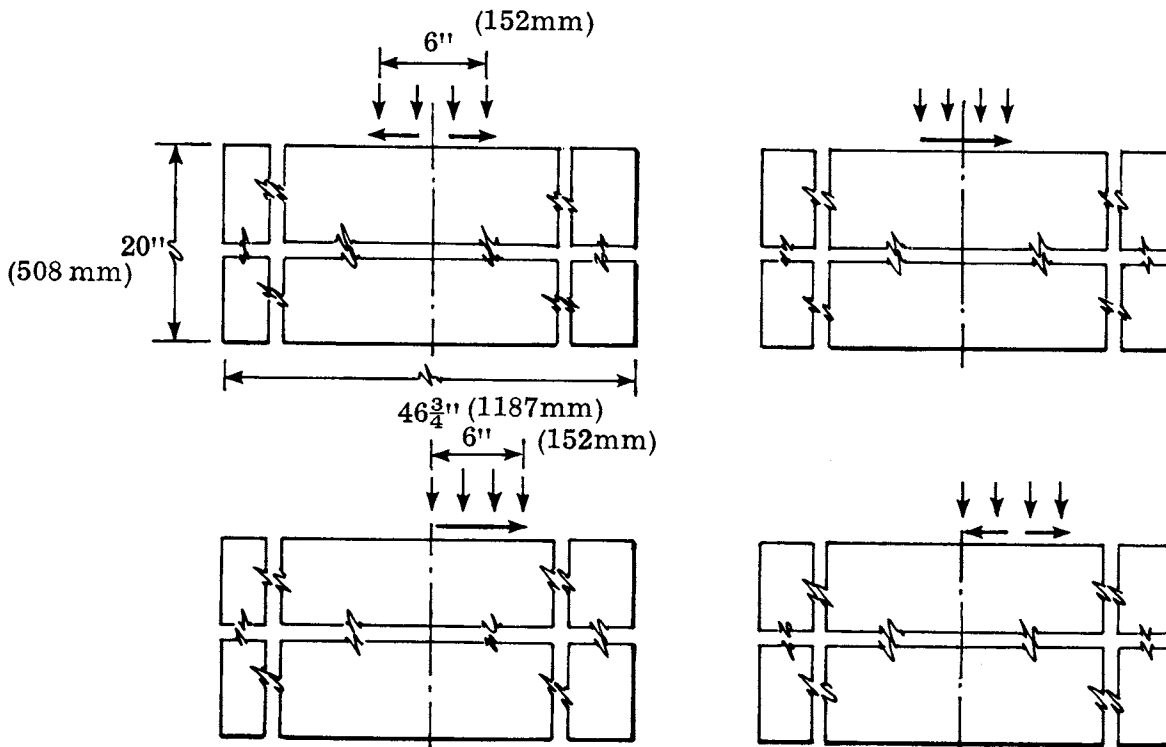


Figure 15. The total system was loaded as shown to obtain the boundary conditions for the small system.

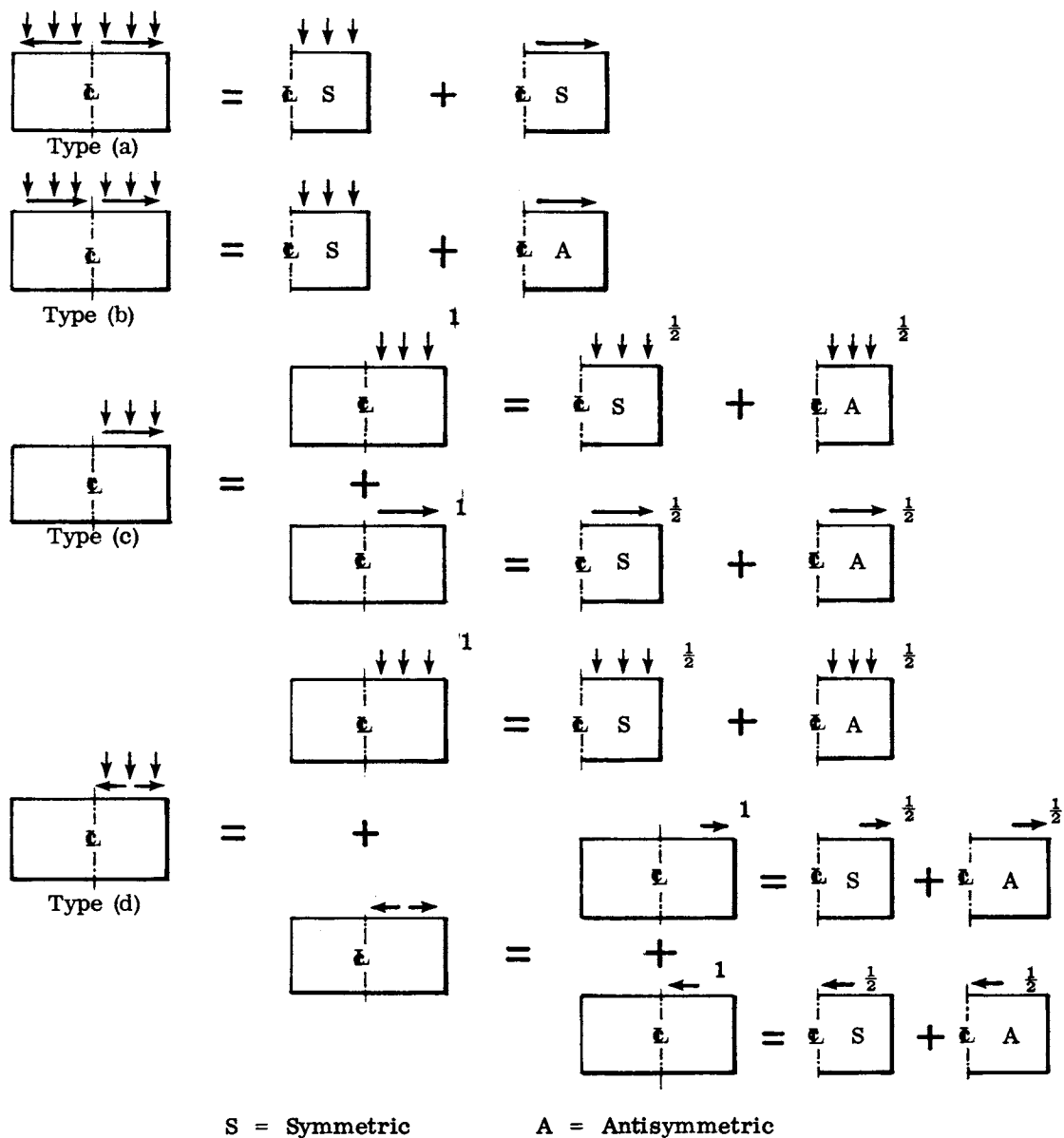
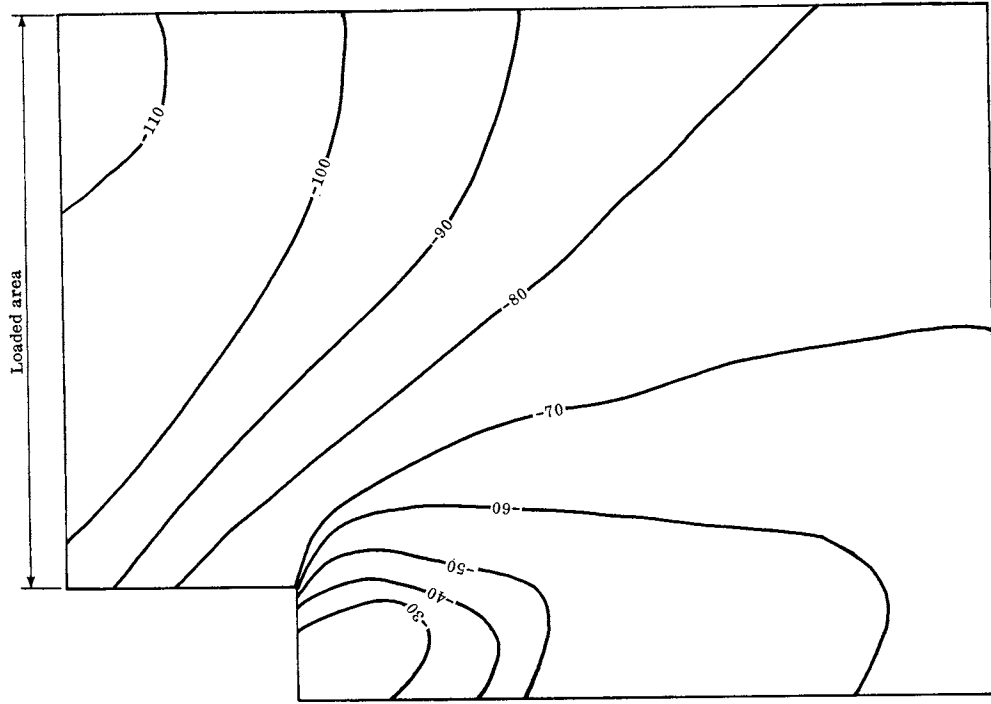
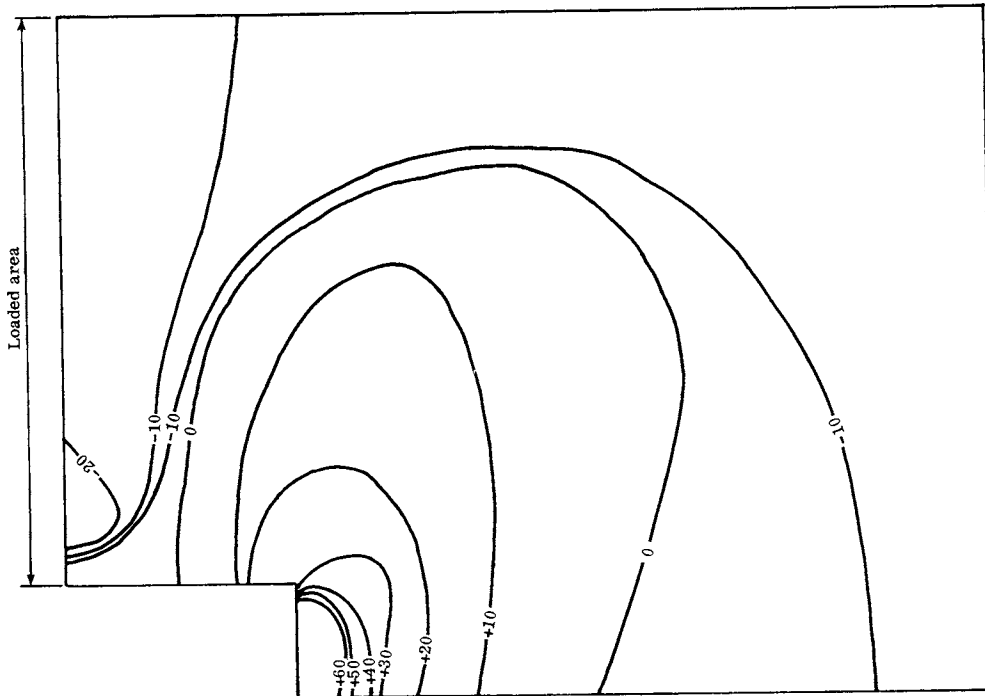


Figure 16. Superposition was used to obtain the boundary conditions and the stresses under the different loading conditions given in Figure 14.



**METRIC EQUIVALENTS**

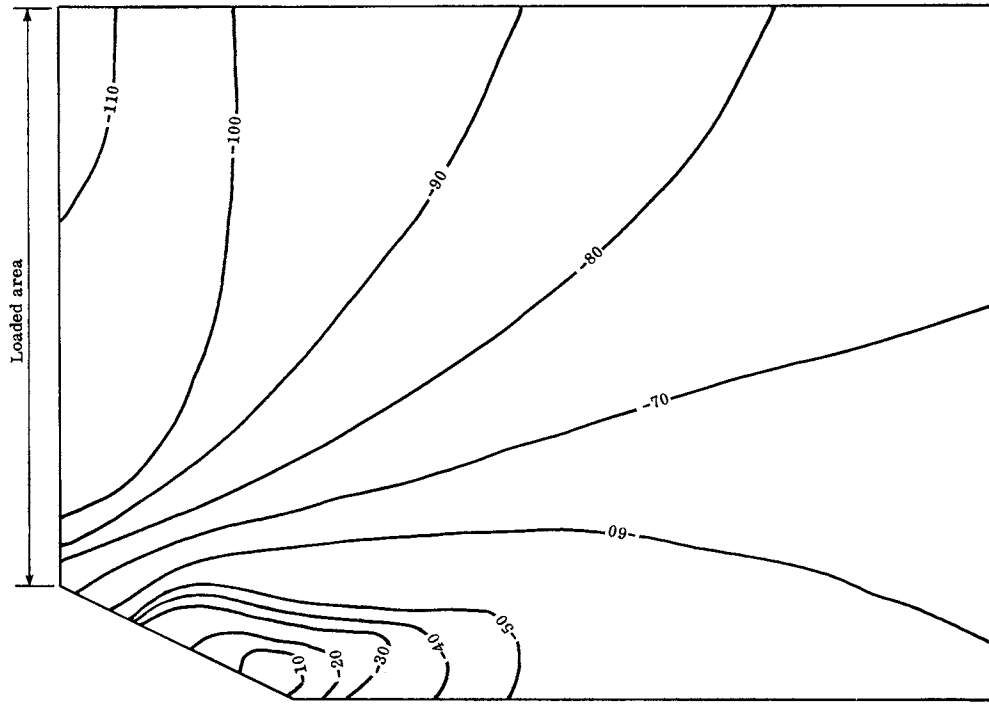
psi	kPa
10	69
20	138
30	207
40	276
50	345
60	414
70	483
80	552
90	621
100	689
110	758
120	827
130	896
140	965
150	1034
160	1103
170	1172
180	1241



Square groove under 100 psi normal and 25 psi shear stress.

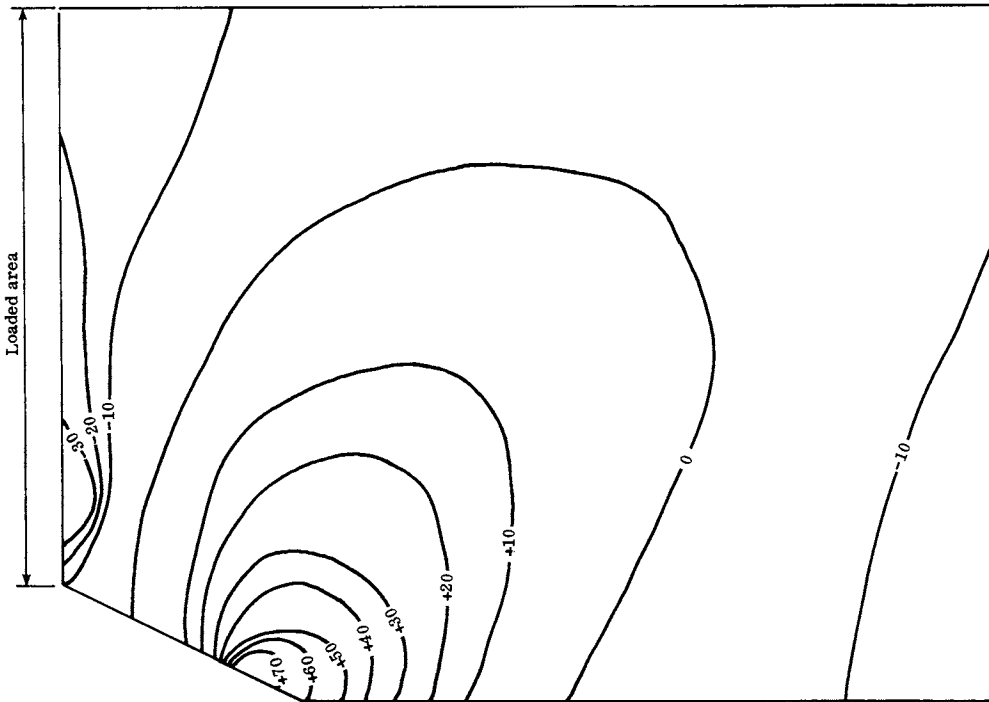
- (+) Principal tensile stresses in psi
- (-) Principal compressive stresses in psi

Figure 17. Stress contours showing the distribution of principal stresses  $\sigma_1$ , and  $\sigma_2$ .



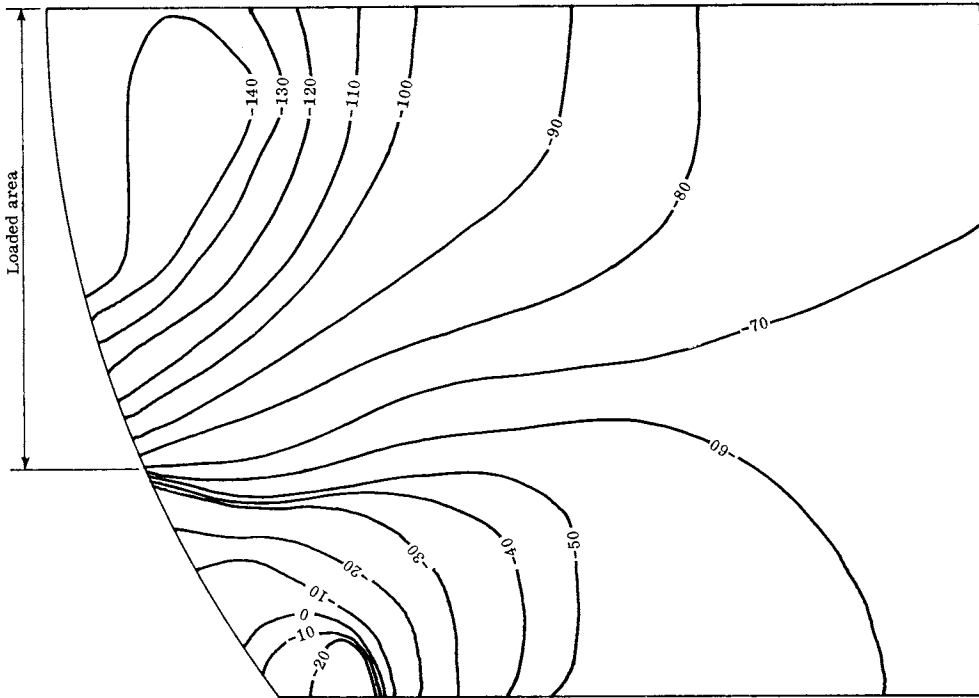
**METRIC EQUIVALENTS**

psi	kPa
10	69
20	138
30	207
40	276
50	345
60	414
70	483
80	552
90	621
100	689
110	758
120	827
130	896
140	965
150	1034
160	1103
170	1172
180	1241



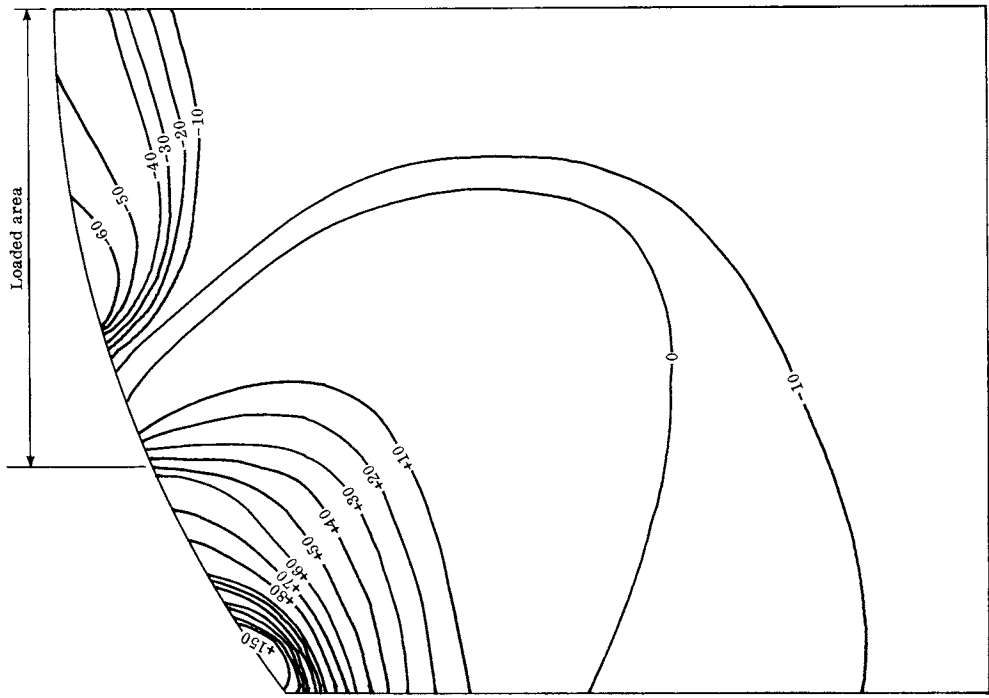
Triangular groove under 100 psi normal and 25 psi shear stress.

Figure 17 (continued)



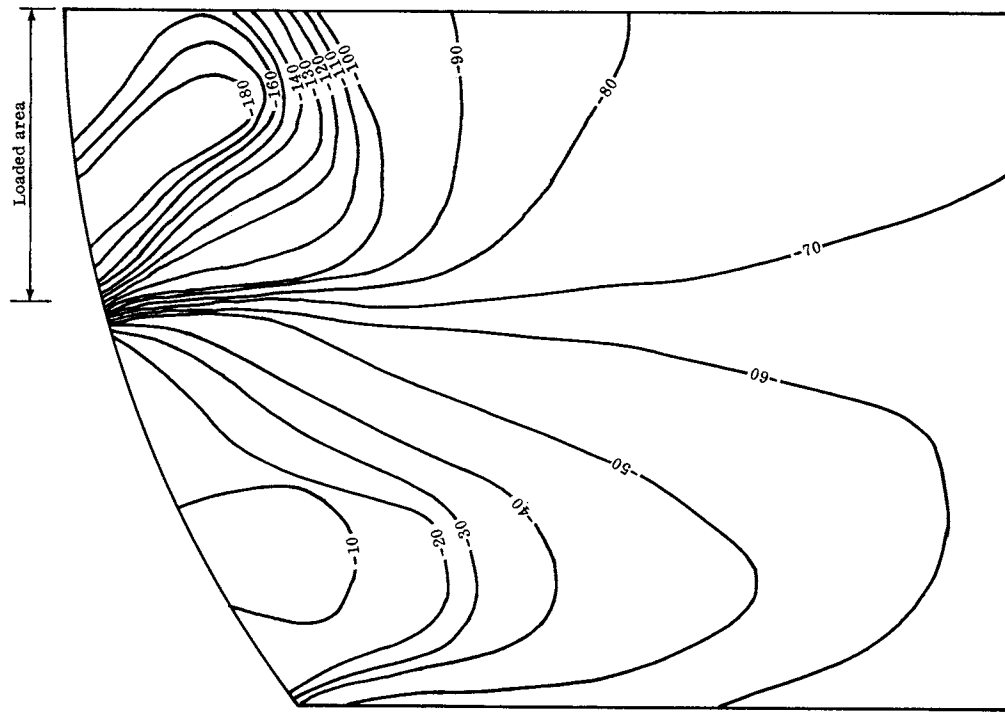
METRIC EQUIVALENTS

psi	kPa
10	69
20	138
30	207
40	276
50	345
60	414
70	483
80	552
90	621
100	689
110	758
120	827
130	896
140	965
150	1034
160	1103
170	1172
180	1241



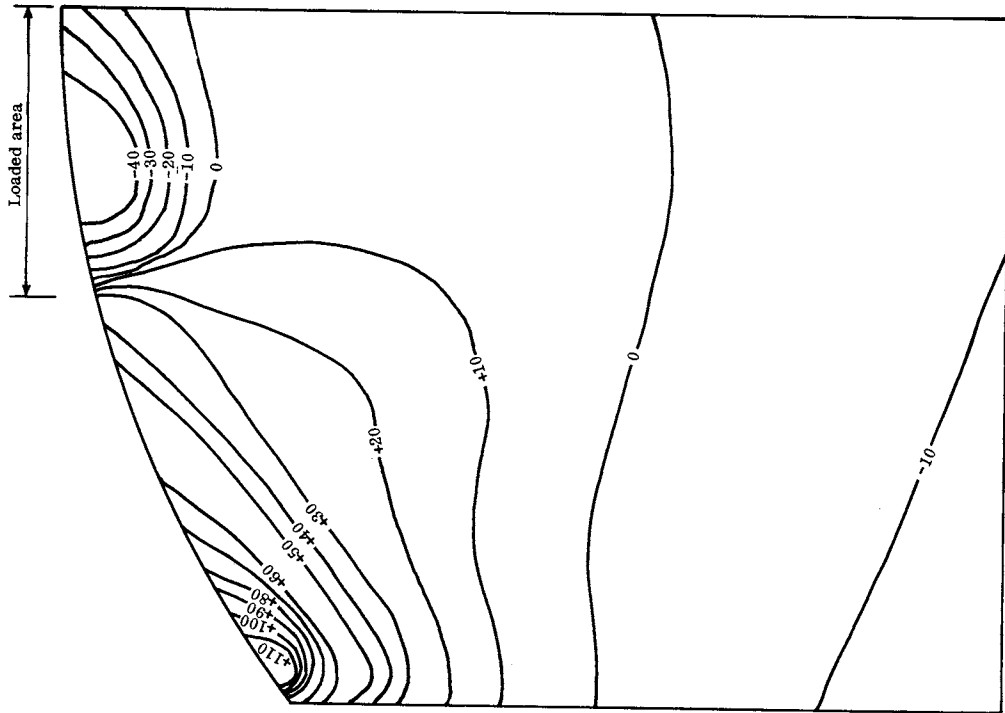
Round groove under 125 psi normal and 31 psi shear stress.

Figure 17 (continued)



METRIC EQUIVALENTS

psi	kPa
10	69
20	138
30	207
40	276
50	345
60	414
70	483
80	552
90	621
100	689
110	758
120	827
130	896
140	965
150	1034
160	1103
170	1172
180	1241



Round groove under 200 psi normal and 50 psi shear stress.

Figure 17 (continued)

The high tensile stresses generated by these two loadings occurred at the bottom and at the corners of the grooves, but they were all below the magnitude sufficient to cause failure by static overstressing. The highest compressive stresses were found at the top surface under loading, but they were very low compared to the ultimate compressive strength of concrete.

The surface shear loading was increased to 75 psi (517 kPa), and all types (a, b, c, d) of loading were used for the square groove, which was intended for comparison with the experimental study. Type (a) loading, which gave high tensile stresses in the initial run, and type (b) loading, which would occur while cornering, were used for all surface configurations.

In this second run for the type (a) loading, zones with high tensile stresses which exceeded the tensile strength of concrete were observed at the bottom of the grooves. In order to study the influence of a sharp corner, the bottoms of the square grooves were rounded to eliminate sharp corners, and the stress values obtained using type (a) loading still had tensile values higher than the tensile strength of the concrete. When type (c) loading with 75 psi (517 kPa) shear was applied to the square groove, tensile stresses close to, but below, the tensile strength of concrete were obtained. Again these high tensile stresses were either at the bottom or at the corners of the grooves. For all types of loading except type (a), tensile stresses were observed at the shoulder of the groove or the top surface, but these were less than 30% of the ultimate tensile strength and therefore not high enough to cause direct failure.

In the type (a) loading, which gave high tensile stresses at the bottom corner of the grooves, the square groove yielded the lowest tensile stress values compared to the other grooves investigated. This finding suggested that the square groove, compared to the triangular and the round groove patterns of this study, would be the most desirable shape. The square groove is easy to make in the concrete and also provides:

- (1) More contact surface than the round groove, which enables a higher adhesion component of friction; and
- (2) larger drainage capacity than the triangular and the round groove, which minimizes hydroplaning.

To investigate the effect of groove geometry on the internal stresses, the depth of the rectangular groove was increased from 1/8" (3.2mm) to 1" (25.4mm) in 1/8" (3.2mm) increments while keeping the groove width and spacing constant so that deeper rectangular grooves were formed. Because of computer storage limits, stresses for only one-half of the rectangular groove were investigated. Different boundary conditions and surface loadings were studied as shown in Figure 18.

Along the centerline of the groove, symmetric and antisymmetric boundary conditions were prescribed. The symmetric one (Cases B and C in Figure 18) represents the type (a) loading whereas the antisymmetric one (Cases A and D) represents the type (b) loading. The side of the groove was initially

restrained from horizontal displacement and then left free to move. The actual situation on the highway is somewhere between the two cases: free movement and no movement.

The surface loading on the system was taken as a 25 psi (172 kPa) shear and 100 psi (689 kPa) normal loading. Then the shear loading was increased to 75 psi (517 kPa), the normal pressure was kept at 100 psi (689 kPa).

The principal tensile stresses which were obtained for an element near the corner of the groove (the location where high principal tensile stresses are computed) versus the depth of groove are shown in Figure 18. The plot indicates that increasing the depth of the groove yields higher principal tensile stresses and that there are two important factors affecting the internal stresses. One of the factors is the action of the shear loading and the other is the boundary conditions. In Figure 18 the plotted lines show the effect of higher shear loading, which causes higher principal tensile stresses. However, it is noted that the effect of shear loading is not apparent when the side of the groove is restrained from horizontal movement (cases C and D). In such a case, the loads are mainly transferred to the reactions and their effects are small around the grooves. When the sides are free to move, higher tensile stresses are developed.

From Figure 18, it is concluded that the deeper grooves are more prone to structural failure, and the two main factors involved are the surface shear loading and the boundary conditions.

#### CORRELATION OF THEORETICAL AND THE EXPERIMENTAL ANALYSES

The theoretical study showed that for 100 psi (689 kPa) normal and 25 psi (172 kPa) shear loading, the stresses around the grooves and the top surface were well below the ultimate capacity of concrete both in tension and compression. When the shear load was increased to 75 psi (517 kPa), the tensile stresses at the bottom and corner of the grooves exceeded the ultimate capacity of concrete. Thus, failure resulting from overstressing would be expected at those locations if the assumed theoretical model with such surface loading and material properties were correct. At the top surface principal stresses were much smaller than the ultimate capacity of concrete. However, in the experimental analysis the specimens obtained from the highways which included a saw cut square groove showed that most of the cracks and wear occurred at the shoulders and at the top surface and resulted in elimination of the microtexture. Hardly any cracks were observed at the bottom of the grooves, which indicated that wear is a surface phenomenon for shallow grooves studied (maximum groove depth of 1/8" (3.2mm)) and that a structural failure associated with large-scale material loss is not expected for such grooves.

Since the theoretical model did not predict the wear observed, other explanations were investigated. The cracks at the top surface were usually parallel and close to the surface. Similar behavior is observed in the wear of metal. This

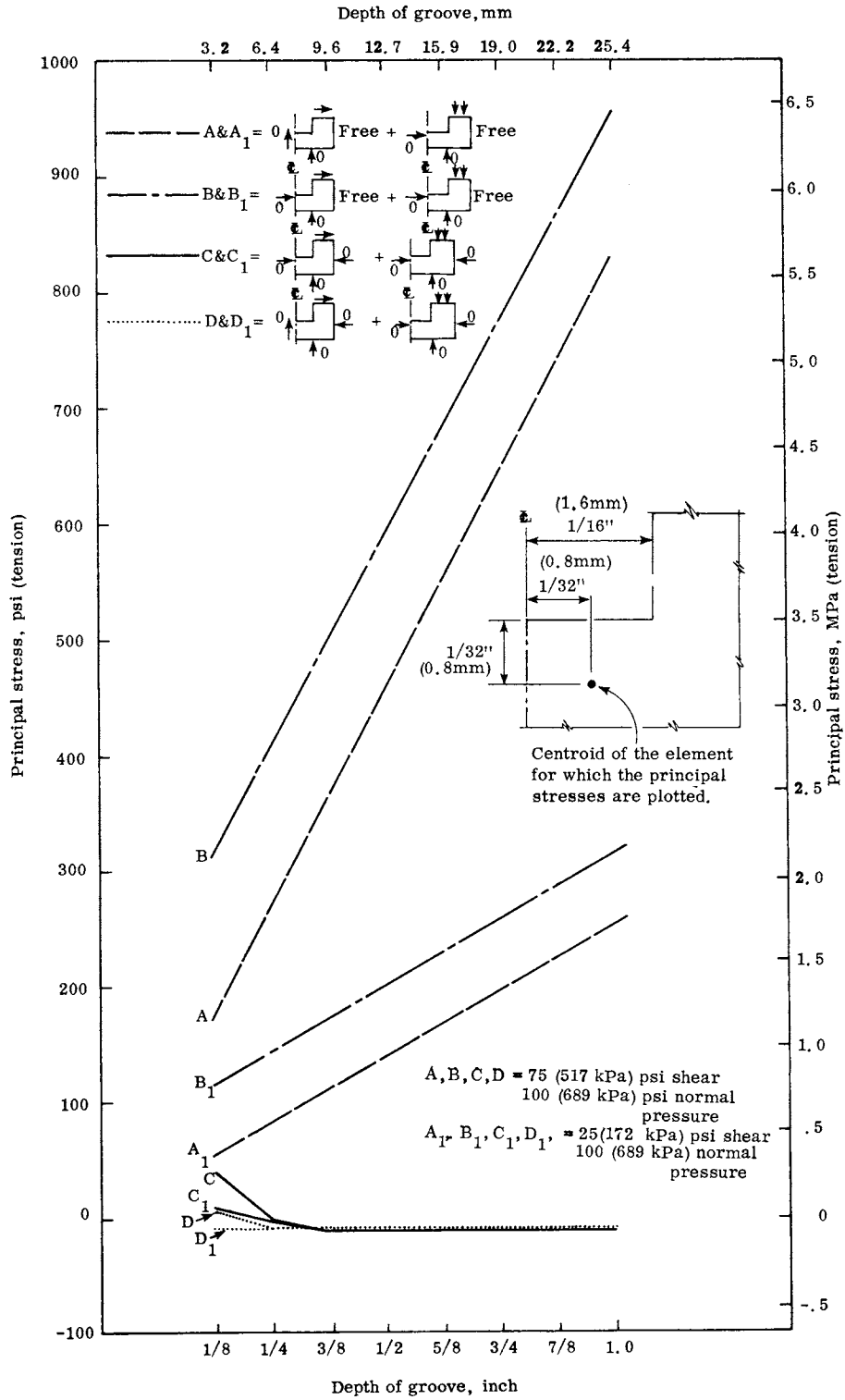


Figure 18. The effect of deeper rectangular grooves on the internal stresses for different loading and boundary conditions.

phenomenon is explained in terms of the occurrence of shear stresses which initiate cracks beneath the contact area between two ideal elastic bodies with curved surfaces pressing against each other. The solution to this problem was obtained by Hertz.(35) The application of the method to concrete assuming an elastic modulus of  $3.2 \times 10^6$  psi (22.1 GPa) and a Poisson's ratio of 0.17, and rubber with an elastic modulus of 100,000 psi (689 MPa) and Poisson's ratio of 0.5, resulted in a crack depth of 8.1 mm, which is almost 40 times deeper than the observed approximate crack depth of 0.2mm in the samples. In the analysis the tire was assumed to have a double radii of curvature of 11" (279 mm) and 13.5" (343mm) carrying a load of 5,000 lb. (2,268 Mg) and the concrete surface was taken to be flat. Because of the inability to explain the mode of failure through the Hertzian contact stress considering the whole tire another approach was pursued.

Due to the asperities and loose material such as grit on the surface, a higher surface loading occurs at certain points. For example, if there is an aggregate protruding at the surface or lying on the surface, the tire arches over it. The arching action results in a larger area of tire load to be carried by a smaller area of the aggregate. The aggregate, because of its size, could transmit the tire load as a concentrated load. If a concentrated load of 500 lb (227 kg) could be transmitted to the surface, a vertical normal stress of 3,900 psi (26.9 MPa) and a principal normal stress of 5,400 psi (37.2 MPa) in compression would occur. The above stress values were obtained at the top surface of the square groove loaded 1/8" (3.2mm) from the side of the groove. The distribution of stresses in the material beneath the load indicated a sharp increase as the surface was reached. The occurrence of high stresses at the top surface confirms that wear involves a surface phenomenon as observed on the pavements experimentally. The loss of material might be due to overstressing or cyclic loading depending upon the heterogeneity of concrete and the magnitude of the load transmitted to the surface.

The new pavement surfaces examined experimentally exhibited a large number of asperities, while the worn surfaces exhibited fewer. As the tire rolled the initial asperities might have been worn to expose some new asperities but not as many as the initial ones. The asperities, whether paste or aggregate, would break off because of high localized stresses. The aggregates might also exert pressure on the paste and initiate cracks. In Figure 3 the flat paste surface on the right-hand side of the asperity in the middle right picture is an apparent continuation of a paste aggregate interface which is mostly outside the picture frame (only a very small portion of the aggregate is visible at the extreme right-hand edge of the frame). This aggregate particle or the aggregate paste interface may have initiated the crack shown in the picture, or the crack might be the result of the stress concentration in the asperity itself. Figure 3 shows a smooth surface without any apparent asperity. The aggregate on the left-hand side of the bottom right picture might have initiated the crack shown. The cause of the surface cracks, their origin and direction of travel were usually hard to determine since the related surface material had been lost, and thin sections would not necessarily indicate the continuous nature of the cracks.

It is conceivable that the asperities could create a wedge action and cause the material underneath to fail. However, no such evidence was observed in the samples studied.

The performance of deeper rectangular grooves which would provide better drainage was investigated. It was found that the deeper grooves are more prone to structural failure since increasing the groove depth would generate higher tensile stresses in concrete as shown in Figure 18. For better drainage another alternative would be to widen the grooves. However, this would result in a decreased contact surface, which is undesirable because of a reduced adhesion component of friction.

### CONCLUSIONS

- (1) Wear observed on the core samples studied was mainly a surface phenomenon. Shoulders and the top surface of the various textures exhibited cracks and loss of material, whereas the bottoms of the grooves were virtually unaffected as observed in the petrographic analysis. The shoulders wore faster than did the top surface.
- (2) The pastes, depending on their quality, disintegrated either by flaking or crushing. Flaking was observed in strong pastes and crushing in weaker pastes, yet both maintained good microtexture. Aggregate, by chipping off at planes and zones of weakness, provided good microtexture. The continuous removal of the small pieces of aggregate and paste at the surface lead to an appreciable decrease in macrotexture (elimination of grooves).
- (3) Both the longitudinal grooves and the transverse grooves indicated the same wear mechanism.
- (4) Durability of the configurations, (round, square, and triangular grooves) as indicated by freezing and thawing in the presence of deicers but in the absence of traffic, was satisfactory and after 50 cycles the differences in the durability of the various groove configurations could not be distinguished.
- (5) A new pavement surface exhibits a weak paste at the very top as seen on the samples from I-64 in New Kent County. Progressive wear results in the wearing away of the weak top surface and exposure of the stronger paste underneath as observed in an older pavement on I-95.
- (6) The theoretical analysis of the internal stress distribution for the round, square, and triangular grooves showed that a structural failure in concrete would be due to the principal tensile stresses occurring at the bottom and corners of the grooves rather than at the surface where the tensile stresses are smaller. However, the stresses determined from 25psi (172kPa) shear and 100 psi (689 kPa) normal loading were not of sufficient magnitude to cause a structural failure.
- (7) Square grooves would serve as the desired pattern compared to the triangular and the round groove patterns of this study. The square groove provides more contact surface than the round groove and thus allows a higher adhesion component of friction. Also it provides a greater drainage capacity than the triangular and the round groove thereby and minimizes hydroplaning.

- (8) The depth of the square groove was studied by the finite element analysis to determine the effect of geometry on internal stresses. A limiting depth of the groove based on the theoretical stress analysis can be determined from Figure 18 depending on the loading and the boundary conditions.

### SUGGESTED FURTHER RESEARCH

A better understanding of the surface loading would be helpful in dealing with tire-pavement interactions. The surface pressure distribution in the presence of grooves and small asperities should be investigated. Additional beneficial information may be gained by various photoelastic procedures including model studies incorporating frozen stress patterns and slice analysis techniques.

It is very hard to simulate the wear of actual highways in the laboratory in a theoretical study. In the laboratory, speeds significantly lower than those on even lightly traveled highways are maintained. In addition, the wear process is slow and it takes a large number of wheel passes to wear the surface. Consequently, it would be beneficial to pursue field studies of different surface textures. Various surface configurations with varying material properties should be imparted to a test section in the highway and exposed to traffic. The comparison among the configurations would indicate the performance of one relative to the others under the existing conditions.

Wheels exert dynamic loads on the pavement. A laboratory study that places cyclic loads on the specimens may yield a better correlation to repeated tire passes on the highways than will a slow moving tire.

Increased rough texture may cause excessive road noise and tire wear. This possibility should be considered in further investigations.

### RECOMMENDATIONS

The top surface of concrete is usually weak because of finishing operations or bleeding. Therefore, it should be recognized that a thin surface layer (about 0.5 mm deep depending upon the quality of concrete) will wear off fast.

The air, water, and cement content of the mix should be carefully controlled to obtain a good quality mixture.

In finishing, the tine spacings should be wide enough to enable the exposure of coarse aggregates near the top surface.

The aggregates should have zones and planes of weakness where pieces would break off and expose a new microtexture. However, this process must be slow to provide long service life. Among the best aggregates for this purpose are certain quartzites and granites.



## ACKNOWLEDGEMENTS

The author is indebted to Jack H. Dillard, head of the Virginia Highway Research Council, and to the FHWA for the facilities and the funding that made this investigation possible.

Sincere appreciation is expressed to Howard H. Newlon, assistant head of the Council, for his suggestion of the topic and for his continuous encouragement, motivation, and generous help at every phase of the study. The author gratefully acknowledges the close supervision of Dr. Richard L. Jennings. Thanks are given to Hollis Walker for the invaluable help in interpreting the thin sections. The author wishes to thank David Mahone, Dr. Fred McCormick, Dr. Kenneth Murray, and Dr. William Zuk for their generous assistance.

The author also extends his thanks to the personnel of the Virginia Highway Department who assisted in various stages of the project.

Special thanks are given to Clyde Giannini, Lewis Woodson, John Stulting, Bobby Marshall, and Jimmie Mills for their valuable help in the experimental phase of this study, and to Cheryl Martin for the typing of the manuscript.



## REFERENCES

- (1) Stone, K. A., "Elements of Skidding", Proceedings, First International Skid Prevention Conference, Virginia Council of Research and Investigation, Part I, p. 1, 1959.
- (2) Colley, B. E., Christensen, A. P., and Nowlen, W. J., "Factors Affecting Skid Resistance and Safety of Concrete Pavements", Special Report 101, Highway Research Board, Washington, D.C., 1969, pp 80-99.
- (3) Mills, J. P., Jr., and Shelton, W.B., "Virginia Accident Information Relating to Skidding", Proceedings, First International Skid Prevention Conference, Virginia Council of Research and Investigation, Part I, p. 9, 1959.
- (4) "Skid Resistance", NCHRP Synthesis 14, Highway Research Board, Washington, D.C., 1972.
- (5) Csathy, T.I., Burnett, W. C., and Armstrong, M.D., "Research on Skid Resistance", Report R.B. 114, Department of Highways, Ontario, Canada 1964.
- (6) Kummer, H.W., and Meyer, W.E., "Tentative Skid Resistance Requirements for Main Rural Highways", NCHRP Report 37, Highway Research Board, Washington, D. C., 1967.
- (7) Kummer, H.W., and Meyer, W.E., "Skid or Slip Resistance", Journal of Materials, Vol. 1, No. 3, September 1966, pp. 667-688.
- (8) Kummer, H.W., and Meyer, W.E., "Rubber and Tire Friction", Engineering Research Bulletin B-80, The Pennsylvania State University, Pennsylvania, December 1960.
- (9) Ludema, K.E., and Gujrati, B.D., "An Analysis of the Literature on Tire-Road Skid Resistance", STP 541, American Society for Testing and Materials, Pennsylvania, July 1973.
- (10) Horne, W.B., and Dreher, R.C., "Phenomena of Pneumatic Tire Hydroplaning", NASA TN D 2056, Langley Research Center, Hampton, Va., November 1963.
- (11) Horne, W.V., and Joyner, V. T., "Pneumatic Tire Hydroplaning and Some Effects on Vehicle Performance", Automotive Engineering Congress, Detroit, Michigan, Jan. 11-15, 1965, Society of Automotive Engineers, Inc., New York, N.Y.
- (12) Allbert, B.J., "Tires and Hydroplaning", Automotive Engineering Congress, Detroit, Michigan, January 8-12, 1968. Society of Automotive Engineers, Inc., New York, N.Y.

- (13) Newlon, H. H., Jr., "Problems Associated with Constructing Skid Resistant Concrete Pavements Using Carbonate Aggregates", Virginia Council of Highway Investigation and Research, Charlottesville, Virginia, December 1962.
- (14) Technical Subcommittee on Surface Properties, "Interim Recommendations for the Construction of Skid-Resistant Concrete Pavement", American Concrete Paving Association and Task Force on Skid Resistance, Portland Cement Association, August 1969.
- (15) Beaton, J. L., "Making Highways Skid Proof", Civil Engineering, ASCE, March 1971.
- (16) Farnsworth, E. E., "Grooving Out Wet Pavement Accidents", Better Roads, Michigan Avenue, Chicago, Illinois, April 1971.
- (17) Weller, D. E., and Maynard, D. P., "Methods of Texturing New Concrete Road Surfaces to Provide Adequate Skidding Resistance", Road Research Laboratory, RRL Report LR 290, Crowthorne, England, 1970.
- (18) Chamberlin, W. P., and Amsler, D. E., "A Pilot Field Study of Concrete Pavement Texturing Methods", Special Report 5, N. Y. State Department of Transportation, Paper at the 51st Annual Meeting of Highway Research Board, Washington, D. C., January 17-21, 1972.
- (19) Lupton, G. N., and Williams, T., "A Study of the Skidding Resistance of Different Tire Tread Polymers on Wet Pavements with a Range of Surface Textures", Paper presented to Symposium on Skid Resistance at Los Angeles, June 1972.
- (20) Sherman, G. B., "Grooving Pattern Studies in California", HRR Number 376, Highway Research Board, Washington, D. C., pp. 11-14, 1970.
- (21) Weller, D. E., and Maynard, D. P., "The Influence of Materials and Mix Design on the Skid Resistance Value and Texture Depth of Concrete", Road Research Laboratory, RRL Report LR 334, Crowthorne, England, 1970.
- (22) Weller, D. E., and Maynard, D. P., "The Use of Accelerated Wear Machine to Examine the Skidding Resistance of Concrete Surfaces", Road Research Laboratory, RRL Report LR 333, Crowthorne, England, 1970.
- (23) Mahone, D. C., and Runkle, S. N., "Pavement Friction Needs", HRR 396, Highway Research Board, Washington, D. C., 1972.
- (24) Spellman, D. L., "Texturing of Concrete Pavements", Special Report 101, Highway Research Board, Washington, D. C., 1969, pp. 100-103.
- (25) Virginia Department of Highways, Road and Bridge Specifications, Commonwealth of Virginia, Richmond, 1970.

- (26) Kerr, P. F., Optical Mineralogy, McGraw-Hill, Inc., New York, 1959.
- (27) Webb, J. W., "The Wearing Characteristics of Mineral Aggregates in Highway Pavements," VHRC 70-R7, Virginia Highway Research Council, Charlottesville, Virginia, November 1970.
- (28) Newman, K., and Newman, J.B., "Failure Theories and Design Criteria for Plain Concrete", Structure, Solid Mechanics, and Engineering Design, Edited by M. Te'eni, Wiley-Interscience, Proceedings of the Southampton, Civil Engineering Materials Conference, 1969.
- (29) 1972 Annual Book of ASTM Standards, Part 10, ASTM, Philadelphia, Pa., 1972.
- (30) Wang, C., and Salmon, C.G., Reinforced Concrete Design, Second Edition, Intext Educational Publishers, New York, 1973.
- (31) Freitag, D.R., and Green, A.J., "Distribution of Stresses on an Unyielding Surface Beneath a Pneumatic Tire", HRB Bulletin 342, Highway Research Board, Washington, D.C., 1962.
- (32) Clark, S.K., Mechanics of Pneumatic Tires, NBS Monograph 122, U.S. Government Printing Office, Washington, November 1971.
- (33) Murphy, G., Advanced Mechanics of Materials, McGraw-Hill Book Company Inc., New York, 1946.
- (34) Rorak, R.J., Formulas for Stress and Strain, McGraw-Hill, Inc., New York, 1965.
- (35) Seely, F.B., and Smith, J.O., Advanced Mechanics of Materials, John Wiley and Sons, Inc., New York, 1952.
- (36) Desai, C.S., and Abel, J.F., Introduction to the Finite Element Method for Engineering Analysis, Van Nostrand Reinhold Company, New York, 1972.
- (37) Hetenyi, M., Handbook of Experimental Stress Analysis, John Wiley and Sons, Inc., New York, 1959.
- (38) Zienkiewicz, O.C., The Finite Element Method in Engineering Science, McGraw-Hill, London, 1971.
- (39) Przemieniecki, J.C., Theory of Matrix Structural Analysis, McGraw-Hill, Inc., New York 1968.
- (40) Rubinstein, M.F., Matrix Computer Analysis of Structures, Prentice-Hall, Inc., Englewood Cliffs, N.J., 1966.
- (41) Clogh, R.W., "The Finite Element Method in Structural Mechanics", Stress Analysis, by Zienkiewicz, O.C. and Hollister, G.E., John Wiley and Sons Ltd., p. 85, 1965.

- (42) Pian, T.H.H., and Tong, P., "Finite Element Methods in Continuum Mechanics", Advances in Applied Mechanics, edited by Chia-Shun Yih, Volume 12, p. 1, University of Michigan, Ann Arbor, Michigan, 1972.
- (43) Martin, H.C., Introduction to Matrix Methods of Structural Analysis, McGraw-Hill, Inc., New York, 1966.
- (44) Beaufait, F.W., Rowan, W.H., Hoadley, P.G., and Hackett, P.H., Computer Methods of Structural Analysis, Prentice-Hall, Inc., Englewood Cliffs, N.J., 1970.
- (45) Timoshenko, S.P., and Gere, J.M., Mechanics of Materials, Van Nostrand Reinhold Company, New York, 1972.
- (46) Utku, S., ELAS 75 Computer Program for Linear Equilibrium Problems of Structures—"User's Manual", Structural Mechanics Series No. 10, School of Engineering, Duke University, North Carolina, December 1971.
- (47) Timoshenko and Goodier, Theory of Elasticity, Second Edition, McGraw-Hill, Inc., New York, 1970.
- (48) Mahone, D.C., "Pavement Friction as Measured by the British Portable Tester and by the Stopping-Distance Method", Materials Research and Standards, American Society for Testing and Materials, Vol. 2 No. 3, pp. 187-192, March 1962.
- (49) Whitehurst, E.A., and Goodwin, W.A., "Tennessee's Method of Laboratory Evaluation of Potential Pavement Slipperiness", Proceedings, International Skid Prevention Conference, Virginia Council of Research and Investigation, Part II, p. 329, 1959.

## LABORATORY SPECIMENS

Fabrication

Twelve textured concrete slabs, as shown in Table A-1 and Figure A-1, were fabricated using skid resistant coarse and fine aggregates. These contained siliceous material that wears slowly and exposes good microtexture. The coarse aggregate was a granite gneiss obtained from the Superior Stone Co., Red Hill, Virginia (Sp. Gr. = 2.79). The fine aggregate was a quartz-sand produced by Lone Star Industries, Inc., Puddleduck, Petersburg, Va. (Sp. Gr. = 2.61 and F.M. = 2.64)

Table A-1

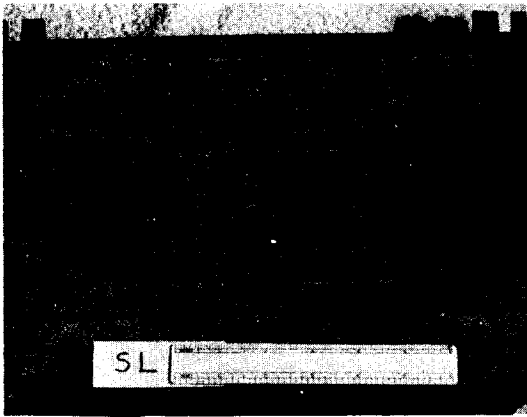
Selected types of textures imparted to the slabs that were tested on the circular test track.

<u>Specimen</u>	<u>Geometry</u>	<u>Orientation</u>
1	Square groove	Longitudinal
2	Triangular groove	Longitudinal
3	Round groove	Longitudinal
4	Square groove	Transverse
5	Triangular groove	Transverse
6	Round groove	Transverse
7	Burlap	Longitudinal
8	Wire brush	Longitudinal
9	Sprinkled chips	
10	Exposed aggregates	
11	Imprinted (fibrous concrete)	Longitudinal
12	Imprinted	Longitudinal

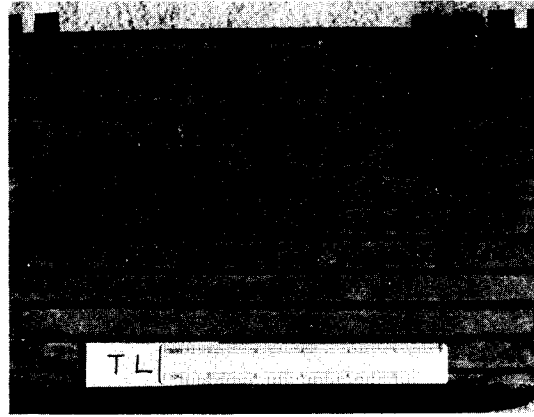
The mixes were designed using the absolute volume method. All the batches except the one for the fibrous concrete were prepared so as to produce similar strengths in accordance with class A-3 mixtures designated by the Virginia Department of Highways. Type II cement was used.

In the case of the fibrous concrete a mixture of 1:2.39: 0.86 by weight having a cement content of 8 bags per cubic yard (445.0 kg per cu. m) with a water-cement ratio of 0.49 was prepared. The amount of fibers in the mix was 200 lbs. per cubic yard (118.4 kg per cu. m). The compressive design strength was 5,000 psi (34.5 MPa). A slump of 2" (50.8mm) and an air content of 6 1/2% was achieved. The slabs had both random and uniform textures. The uniform shapes shown in Figure 11 were obtained by casting concrete on steel molds of the desired groove pattern.

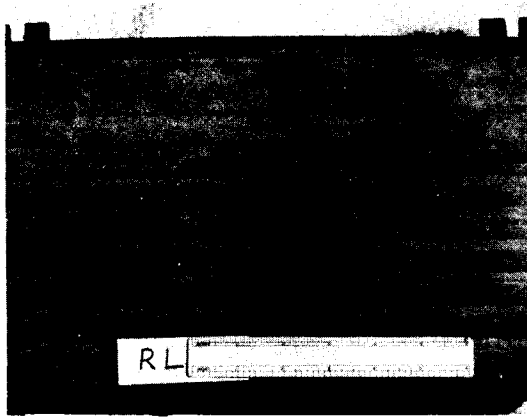
A sensing instrument was located in a specimen having longitudinal grooves to measure the forces occurring at the tire-pavement interface. (Figures A-2 and A-3). These forces were intended to be used in the theoretical analysis as loads exerted on the surface.



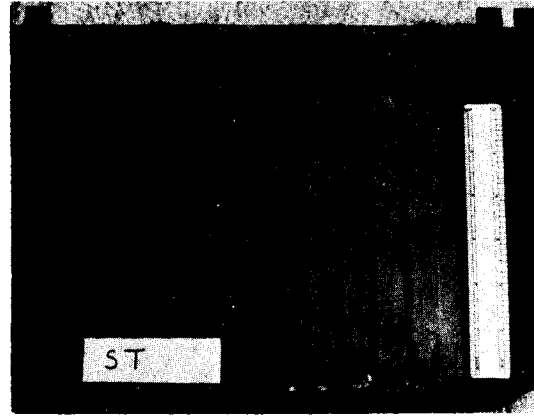
Longitudinal square groove



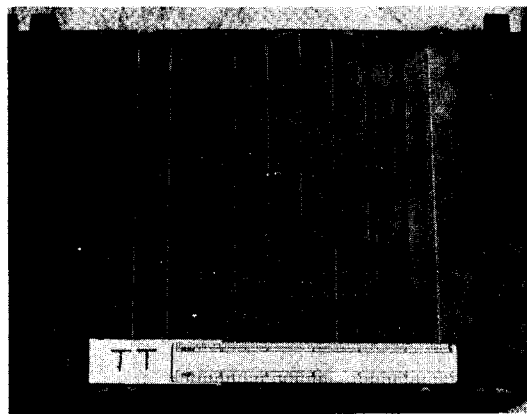
Longitudinal triangular groove



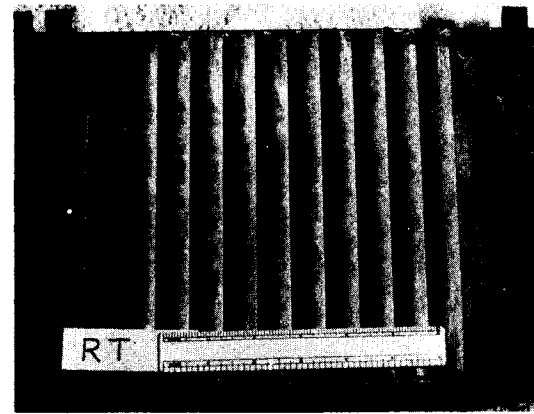
Longitudinal round groove



Transverse square groove

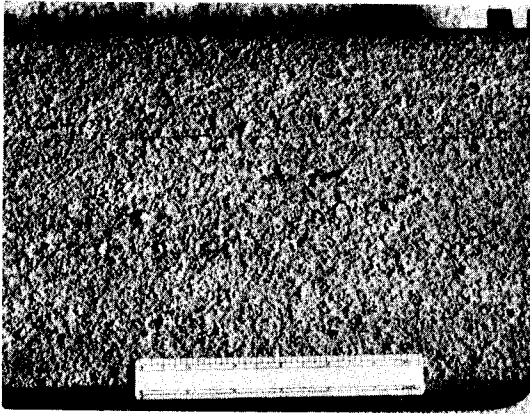


Transverse triangular groove

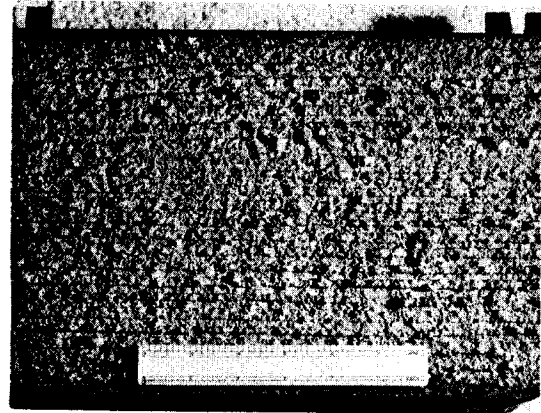


Transverse round groove

Figure A-1. Top view of the concrete slabs with various textures that were subjected to wear at the circular test track.



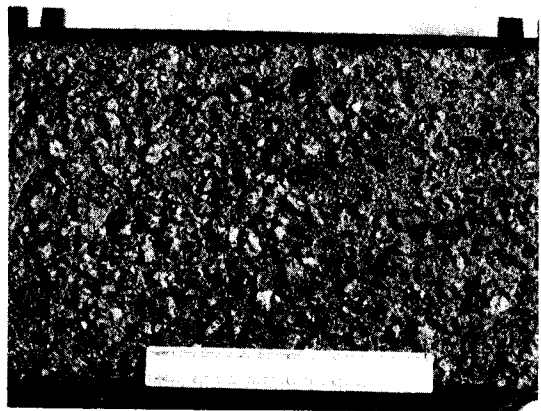
Burlap



Wire brush



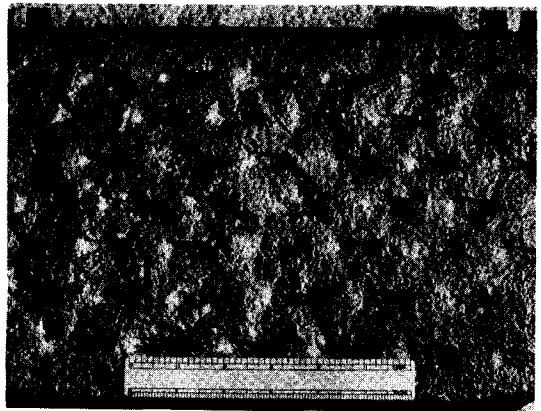
Sprinkled chips



Exposed aggregates



Imprinted (fibrous concrete)



Imprinted

Figure A-1 (continued)

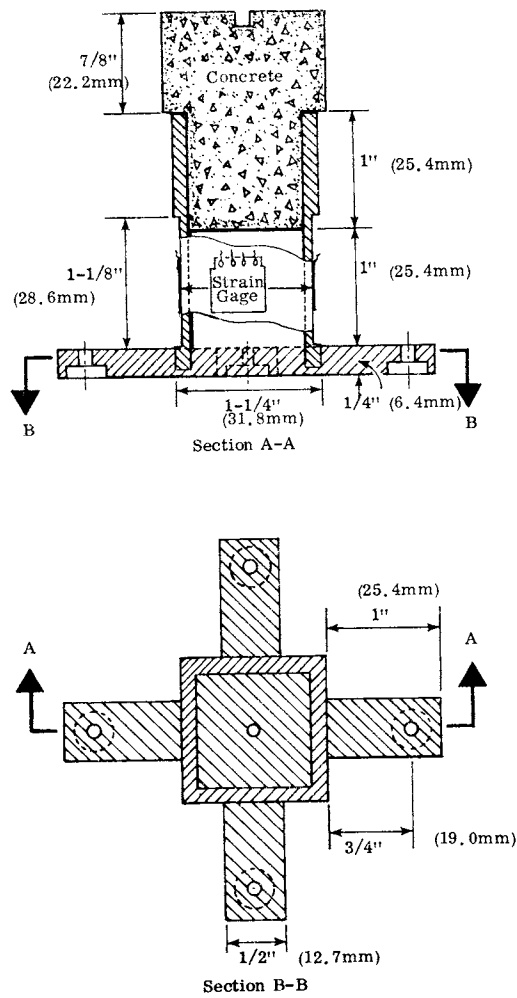


Figure A-2. A sensor was built to measure the surface forces.



Figure A-3. Sensor was set inside the specimen having longitudinal grooves.

### Testing

All the specimens were subjected to wear at the test track of the Maryland Road Commission, shown in Figure A-4, for 835,000 cycles which is equivalent to 1,670,000 wheel passes. The test track is 6' (1.83 m) in diameter with two wheels connected to a central shaft, that rotates in a horizontal plane at 24 rev/min under a 1,000 lb. (454 kg) vertical loading on each wheel.

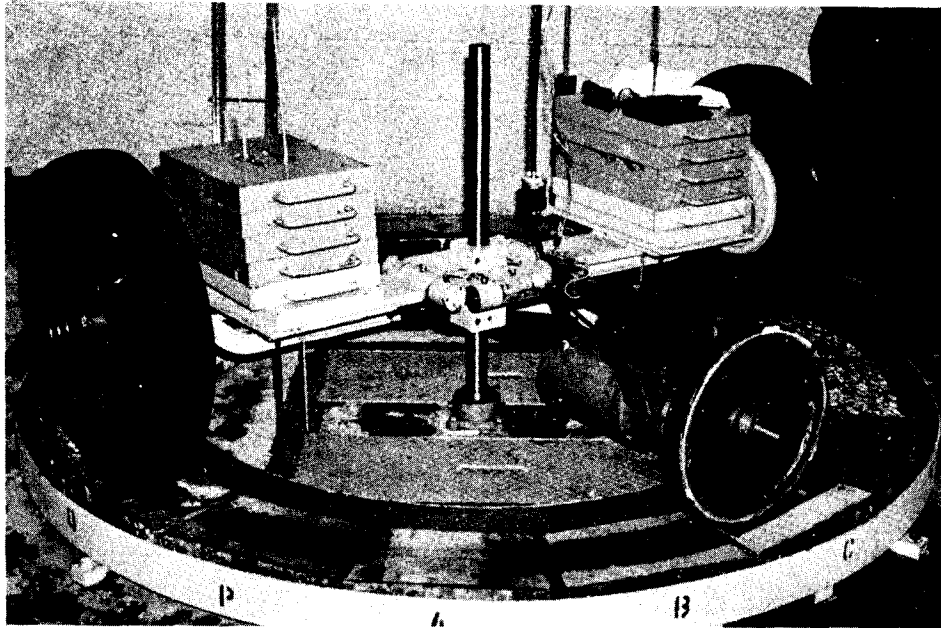


Figure A-4. Circular test track of the Maryland Road Commission used in the experimental phase.

At certain time intervals, skid numbers ( $SN = 100 \times$  coefficient of friction) were obtained with a British Portable Tester (BPT) (48). At each interval an average of four tests was used. The plots are shown in Figures A-5 through A-8. Within the first 100,000 cycles the skid numbers dropped rapidly; afterwards a slight decrease and then a leveling off were observed. The skid numbers measured with the BPT were influenced mainly by the contact area, the microtexture, and the physical interference caused by the orientation of the grooves. The general trend of the curves approximates that shown earlier in Figure 1.

The speed parameter could not be accommodated because of the very low test speed of the BPT, 5 to 7 mph (8 to 11 km/hr). Thus, the beneficial effect of grooves at high speeds was not reflected. The groove spacing decreased the contact area, which caused a decrease in skid resistance. The uniform idealized shapes with longitudinal grooves gave low skid numbers. Because they were cast on a steel mold, they had a smooth surface with poor microtexture. It was originally anticipated that initial tire passes would roughen the surface of uniform shapes and

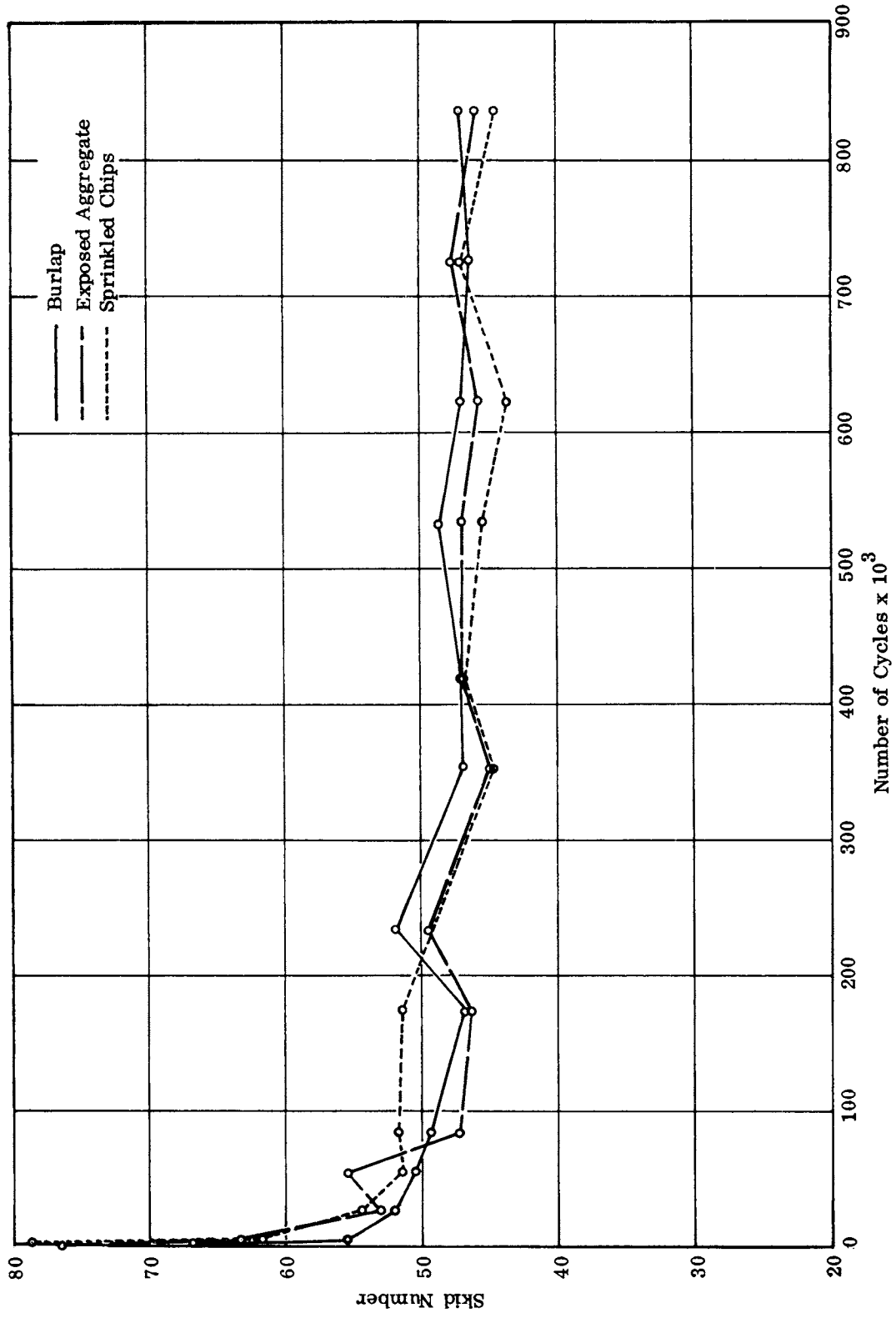


Figure A-5. Skid number vs. number of cycles for the random textures.

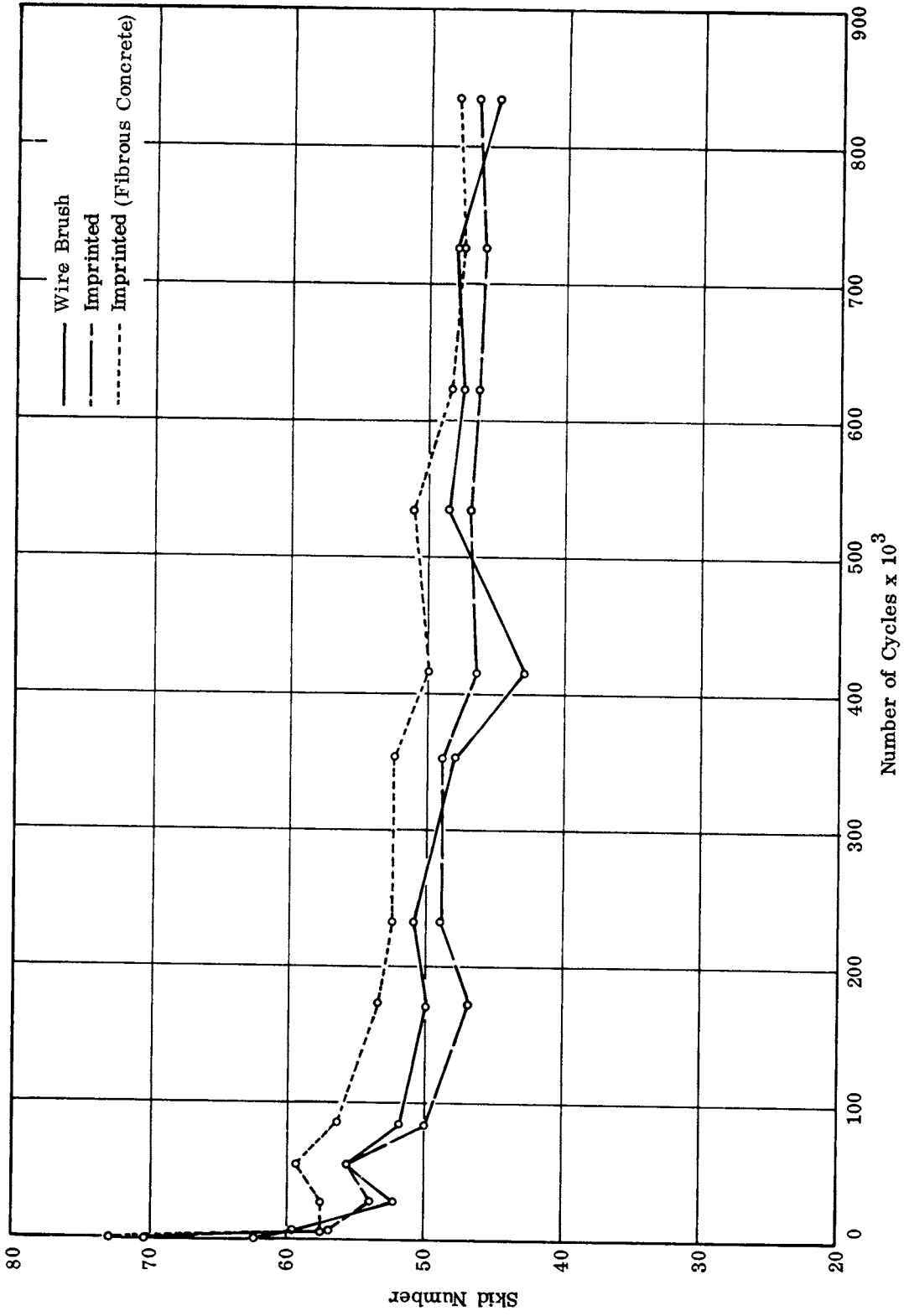


Figure A-6. Skid number vs. number of cycles for the random textures.

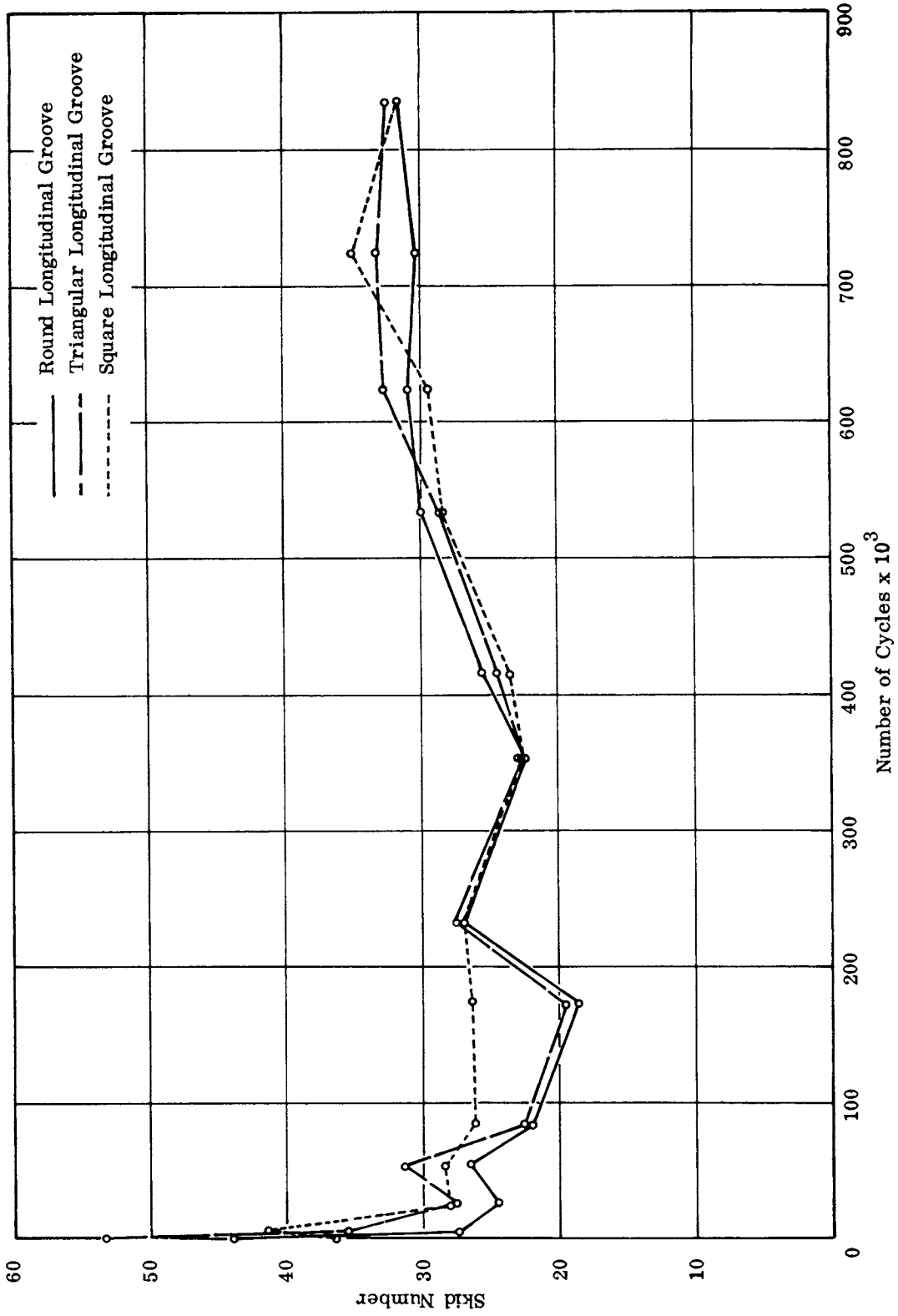


Figure A-7. Skid number vs. number of cycles for the uniform longitudinal grooves.

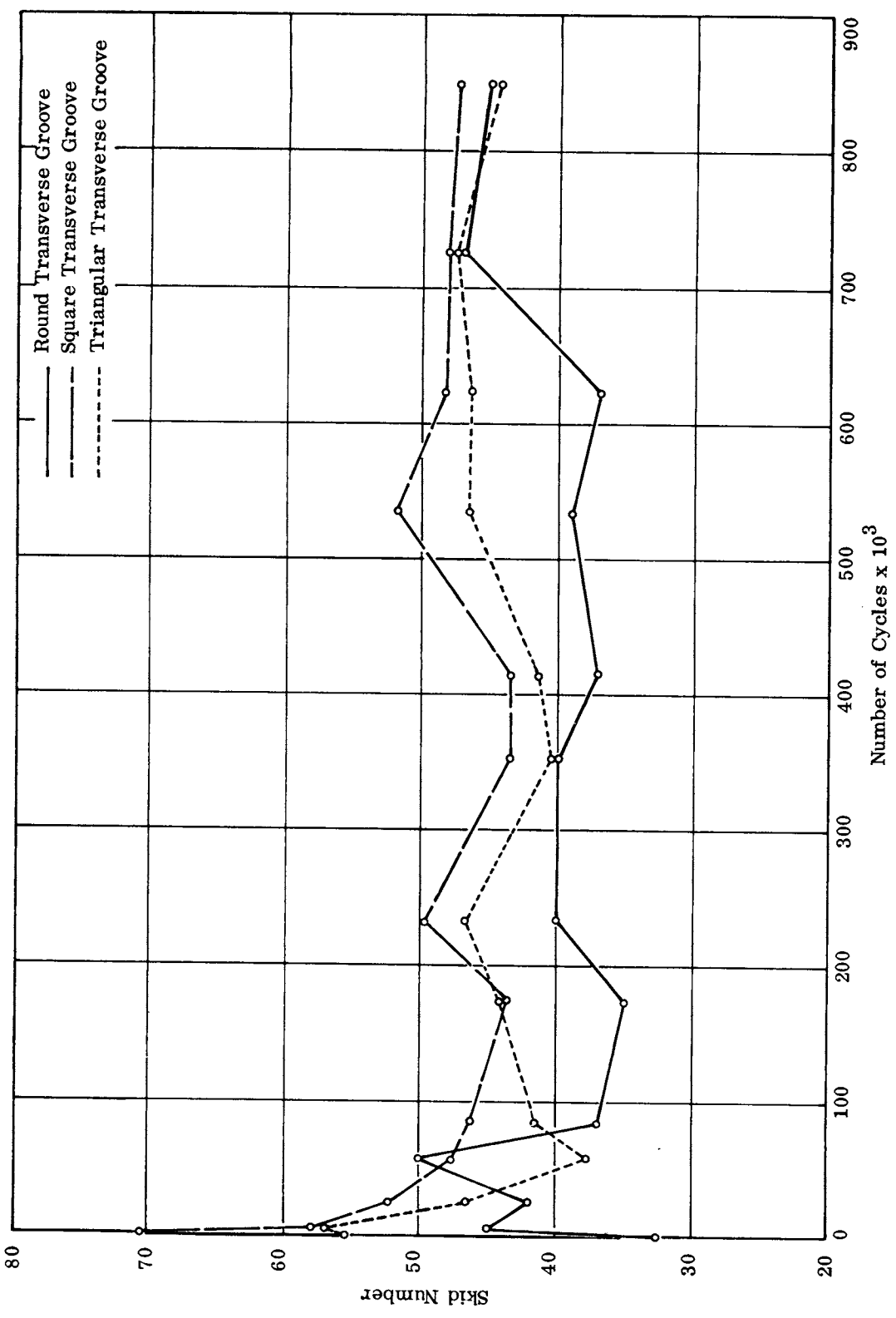


Figure A-8. Skid number vs. number of cycles for the uniform transverse grooves.

a satisfactory microtexture would be achieved. This happened in the case of longitudinal grooves after 500,000 cycles but did not increase the skid numbers appreciably. Uniform transverse grooves gave higher frictional values, probably because of the catching of the rubber slider of the BPT at the grooves. The slab with fibrous concrete showed more resistance than the one with plain concrete and the same texture. The rubber slider might have experienced more resistance because of the protruding wires. The fluctuation of the skid numbers for the same texture at increasing numbers of tire passes might have resulted from the varying microtexture exposed at the time of test.

The sensing device proposed to measure the forces at the tire-pavement interface did not give satisfactory results, since the forces at the surface were very low. In addition, errors resulting from the sticking, vibrating, and squeezing effect of the treads altered the small force components considerably.

The testing of slabs in the test track caused some degree of polishing, but there was no measurable decrease in texture depth. Therefore, the petrographic examination of these slabs was omitted. It is anticipated that utilizing the circular track to obtain a significant decrease in texture depth would take quite a long time, possibly a few years. More rapid wear is gained in the same period in the field on Virginia's heavily traveled pavements.

Because of the difficulties encountered with the use of the circular test track concerning the degree of wear and the measurement of the surface forces, a different type of facility was investigated. This apparatus in Tennessee, shown in Figure A-9, consists of a wheel rotating in a vertical plane at constant speed about a fixed axle.<sup>(49)</sup> The wheel is kept on the specimen under a 270 lb. (122 kg) load. Higher loads cause rapid wear and damage to the rotating tire. The wheel rotates at a constant speed, equivalent to a vehicle's traveling at 10 mph (16 km per hr). The power required to keep this constant speed is recorded. Within a couple hours it is possible to obtain sufficient polishing to cause a slippery surface. However, consultation and some limited testing with this equipment revealed that it is doubtful that a significant decrease in texture depth could be achieved using the rotating wheel. For these reasons the remaining experimental phase of the work was directed and confined to observations on cores removed from pavements in service.

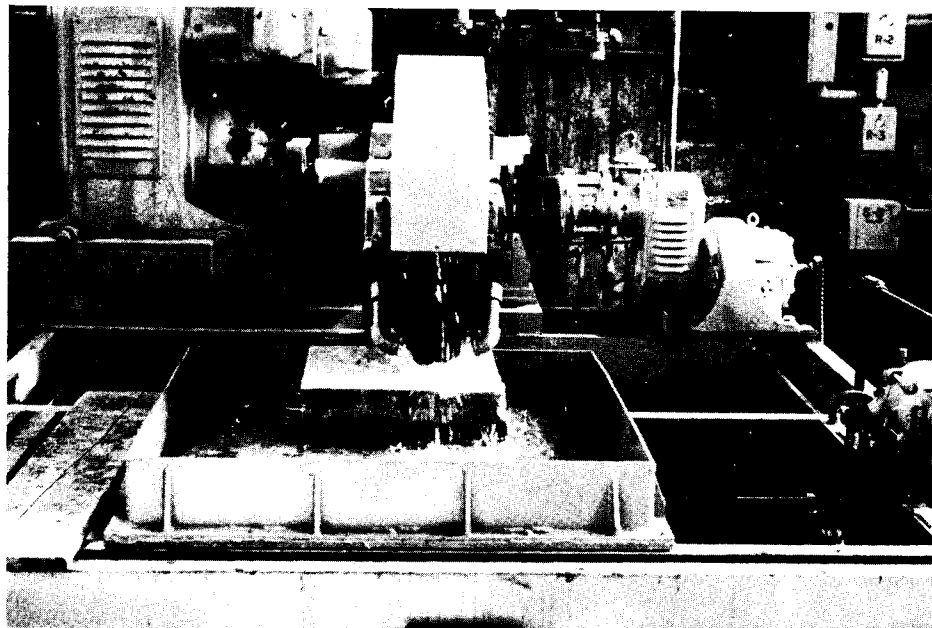


Figure A-9. Test apparatus consisting of rotating wheel.

